Study of the conformational behaviour of trehalose mycolates by FT-IR spectroscopy

F. Migliardo, Y. Bourdreux, M. Buchotte, G. Doisneau, J.-M. Beau, Nicolas Bayan

Version of Record: https://www.sciencedirect.com/science/article/pii/S0009308419301082
Manuscript_449d43c6639d19b276a087f46ba4d652

Study of the conformational behaviour of trehalose mycolates by FT-IR spectroscopy

F. Migliardo [a,b*], Y. Bourdreux[c], M. Buchotte[d], G. Doisneau[c], J.-M. Beau[c,e], N. Bayan[f]

[a]*Department of Chemical, Biological, Pharmaceutical and Environmental Sciences, University of Messina, Viale D'Alcontres 31, 98166 Messina, Italy*

[b]*Laboratoire de Chimie Physique, UMR8000, University Paris Sud, 91405 Orsay cedex, France*

[c]*Synthèse de Molécules et Macromolécules Bioactives, Institut de Chimie Moléculaire et des Matériaux d'Orsay (ICMMO), UMR 8182, Université Paris-Sud and CNRS, Université Paris-Saclay, F-91405 Orsay, France*

[d]*Services Communs, Institut de Chimie Moléculaire et des Matériaux d'Orsay (ICMMO), UMR 8182, Université Paris-Sud and CNRS, Université Paris-Saclay, F-91405 Orsay, France*

[e]*Institut de Chimie des Substances Naturelles, CNRS UPR2301, University Paris-Sud, University Paris-Saclay, 1 avenue de la Terrasse, F-91198 Gif-sur-Yvette, France*

[f]*Institute for Integrative Biology of the Cell (I2BC), CEA, CNRS, University Paris-Sud, University Paris-Saclay, F-91198 Gif-sur-Yvette, France*

Abstract

Mycolic acids are fundamental cell wall components, found in the outer membrane barrier (mycomembrane) of *Mycobacterium* related genera, that have shown antigenic, murine innate immunity inducting and inflammatory activity triggering action. The mycolic acid derivatives, such as the lipid extractable trehalose monomycolates (TMM) and dimycolates (TDM), have been extensively investigated by several biochemical and biological methods and, more recently, we have performed the first neutron scattering measurements on these molecules in order to characterize their dynamical behavior as well as their rigidity properties. In the present paper, we show the first systematic FT-IR study on TMM, TDM and glucose monomycolate (GMM). It

includes the analysis of individual lipids but also mixtures of TMM/TDM (ratio of 1:1) or TMM/GMM (ratio of 1:2).

The present work is aimed to the first characterization of the vibrational behavior of mycolates and their mixtures enabling us to elucidate the molecular mechanisms responsible for the capability of mycolic acids to affect the flexibility and permeability properties of the mycomembrane. As a whole, the present FT-IR findings provide information that have relevant biological implications, allowing to demonstrate that the membrane fluidity is not only linked to the chain length, but also to the specific conformational behavior adopted by mycolates, which in the mixtures is strongly affected by their mutual interactions. In addition, the capability of trehalose to drive the mycolate conformational behavior and then the chain order and packing is emphasized; due to the TDM relevant evidences shown by our data, this trehalose effect could be related to the TDM toxicity and inflammation action.

Keywords: trehalose mycolates; mycomembrane; Infrared spectroscopy; chain order; chain length; fluidity

1. Introduction

According to the World Health Organization, in 2017 there were 10 million of tuberculosis (TB) cases and 1.6 million deaths for TB. Among these latter, 1 million were children; 1.3 million among HIV negative-associated TB and 300000 among HIV positive-associated TB (Global tuberculosis report 2018). In addition, multidrug-resistant (MDR) and extensively drug-resistant (XDR) strains of *Mycobacterium tuberculosis* make tuberculosis an almost incurable disease. Research is therefore strongly addressed towards innovative solutions for reliable and fast diagnostic tools (Wood 2007; Beukes et al. 2010).

Many studies have been devoted to the role of the very specific outer membrane barrier (mycomembrane) found in all mycobacteria related genera (the order of Corynebacteriales) in host

response (Nabeshima et al. 2005; Sekanka et al. 2007), with a particular emphasis to the mycolic acids and their derivatives, such as the lipid extractable trehalose monomycolates (TMM) and dimycolates (TDM). The role of mycolic acids as murine innate immunity inducting and inflammatory activity triggering agents has been also demonstrated (Korf et al. 2005; Korf et al. 2006).

Mycolic acids are α branched and β hydroxylated fatty acids containing a non-functionalized long alkyl chain (up to 60 atoms of carbon) and a "meromycolate chain" generally containing up to two functional groups (Verschoor et al. 2012). Mycolic acids of Corynebacteria are characterized by the shortest chains, i.e. between 28 and 40 carbon atoms, with a permeability barrier which is not essential for the bacterial life in laboratory conditions (Portevin et al. 2004), whereas mycolic acids of mycobacteria show among the largest chains, i.e. between 60 and 90 carbon atoms; chains of intermediate length are typical of Rhodococcus and Nocardia (Hsu et al. 2011; Nishiuchi et al. 1999).

Many biochemical studies highlighted that TDM is capable to affect the mycobacterial morphology (Hunter et al. 2006), to drive phagosome-lysosome fusion in vivo (Spargo et al. 1991), to increase chemokine and cytokine production and to modify immunological response (Ryll et al. 2001), to induce granulomas (Kai et al. 2007), and to prevent phagocytosed bacterial trafficking to macrophage acid regions (Indrigo et al. 2003).

It has been emphasized (Verschoor et al. 2012) that the chemical synthesis of mycolic acids is crucial for understanding the role of these systems in corynebacteria and mycobacteria, since the investigations carried out on natural mixtures of mycolic acids and mycolates do not provide unambiguous evidence on the specific functions of these systems due to the influence of the complex environment, i.e. the interaction among mycolic acids and the other membrane components.

With the ultimate goal of understanding the molecular mechanisms responsible for the capability of mycolic acids to affect the flexibility and permeability properties of the mycomembrane, we carry out a FT-IR spectroscopic study of the vibrational behavior of TMM/TDM mixture at a ratio of 1:1

which has been both extracted from the mycomembrane of *C. glutamicum* and chemically synthetised; measurements have been also performed on individual TMM, TDM and glucose monomycolate (GMM) molecules in order to unambiguously assign the FT-IR spectral features to the vibrational modes of the investigated mycolates. A further comparison was performed between the TMM/TDM mixture and the TMM/GMM mixture at a ratio of 1:2 in order to investigate the role of the trehalose glycosidic bond in the conformational arrangements of the mycolates.

Since the present work is the first FT-IR study on trehalose and glucose mycolates and their mixtures, existing data on lipids and bacteria (Yoshida and Koike 2011; Lewis and McElhaney 2013; Wallach 1972; Lewis and McElhaney 1998; Tamm and Tatulian 1997; Gautier et al 2013; Davis and Mauer 2010; Binder 2007; Naumann et al. 1991; Naumann 2000; Oberreuter et al. 2002) supported the interpretation of the obtained findings also on the light of their biological significance.

2. Experimental section

TMM, TDM and GMM were chemically synthesized. All commercially available chemicals were used without further purification. All air sensitive reactions were carried out in oven-dried glassware under a slight positive pressure of argon. Solvents were distilled according to the literature (Perrin and Armarego 1997) or by filtration through a column of activated alumina using equipment from Glass Technology® (dry solvent station GT S100). TLC (Silica Gel 60 F254) were visualized under UV (254 nm) and by staining either in 5% ethanolic sulfuric acid or orcinol or phosphomolybdic acid. Silica gel SDS 60 ACC 35-70 μm was used for column chromatography. Melting points were measured on a Stuart SMP10 apparatus. NMR spectra were recorded on a Bruker AV 360 NMR spectrometer.

TMM, TDM and GMM were synthesized starting from corynomycolic acid **1** (Ratovelomanana-Vidal et al. 2003) and trehalose derivative **2** (Kurita et al. 1994; Kanemaru et al. 2012) or glucose derivative **3** (Lu et al. 2005), according to previously reported procedures, as shown in Figure 1.

Corynomycolic acid **1** was firstly prepared starting from β-ketoester **4** accordingly to the procedure described by Genêt and Ratovelomanana-Vidal (Ratovelomanana-Vidal et al. 2003) (Figure 2). Briefly, β-ketoester **4** was obtained after a 2-carbon atoms homologation of palmitic acid using the Masamune's procedure. Compound **4** was then selectively reduced with dihydrogen using the Noyori's catalyst i.e. (*R*)-BinapRuBr$_2$. The resulting β-hydroxyester **5** was then engaged in a selective alkylation (LDA, HMPA) with *n*-iodotetradecane at low temperature to furnish the *anti* α-alkylated compound **6**. Saponification of the ester function of compound **6** (KOH, EtOH/H_2O) yielded corynomycolic acid **1**. Spectroscopic data of all compounds were in agreement with those previously reported (Ratovelomanana-Vidal et al. 2003).

Finally, sugar mycolates, GMM, TMM and TDM were subsequently prepared by nucleophilic substitution of the corresponding tosylate groups of **7**, **8** and **9** using the cesium salt of mycolic acid in a DMF/THF mixture at 70°C (Figure 3), followed by hydrogenolysis of the benzyl groups (H_2, Pd/C, MeOH) according to previously reported reports (van der Peet et al. 2015; Prandi 2012). Spectroscopic data were in agreement with those reported (van der Peet et al. 2015). Figure 4 shows the ^{1}H NMR spectra of TMM, TDM and GMM.

From a structural point of view, TMM ($C_{44}H_{84}O_{13}$) is constituted by a double chain of 18 carbon atoms and 14 carbon atoms, which is bonded to a trehalose molecule, TDM ($C_{76}H_{146}O_{15}$) presents two double chains, with 18 carbon atoms and 14 carbon atoms for each, bonded to a trehalose molecule, and GMM ($C_{38}H_{74}O_8$) is composed by a double chain as TMM but bonded to a glucose molecule.

These systems present therefore as functional groups: CH_2 groups (26 for TMM and GMM, 52 for TDM), CH_3 groups (2 for TMM and GMM, 4 for TDM), OH groups (8 for TMM and TDM of which one and two are linked to the acyl chain, respectively, and 5 for GMM of which one is linked to a the acyl chain), CO groups (1 for TMM and GMM, 2 for TDM, in all the cases a double bond exist between C and O) and CO-O-C groups (1 for TMM and GMM, 2 for TDM).

The extraction of TMM/TDM has been carried out starting from a culture of *C. glutamicum* strain ATCC 13032 *ΔaftB*, which releases outer membrane fragments in the external medium (Marchand

et al. 2012). After an overnight culture in liquid brain heart infusion (BHI) medium at a temperature of 30°C, the supernatant culture has been obtained by centrifugation at 6000 g for 20 min and, after a high speed centrifugation at 100000 g, the mycomembrane fragments have been purified. The extraction of lipids, i.e. TMM/TDM at a ratio of about 1 from these membrane fragments has been performed three times with $CHCl_3$-CH_3OH solutions at the volume ratios of 1:2, 1:1 and 2:1 following the procedure described in Marchand et al. (Marchand et al. 2012). The main mycolic acid species of C. glutamicum are of the C32:0, C26:0, C24:0, C34:1, and C35:0 type (Yang et al. 2012; Lanéelle et al. 2013); depending on the strains shorter homologues, i.e. C16:0 to C30:0, can be also present.

FT-IR measurements have been performed by using a Bruker Alpha II spectrometer allowing an advanced stabilization of source and detector against environmental changes. Measurements have been carried out in ATR mode combining a Platinum ATR module equipped with a diamond crystal, at a resolution value of 3 cm^{-1} and covering a frequency range between 400 cm^{-1} and 3500 cm^{-1}. A number of 96 scans has been acquired for each of the two samples investigated for each system. The data collection and the spectra standard reduction (baseline and atmospheric corrections) have been carried out by using the OPUS software. Due to the overlapping of the peaks, the analysis of the complex bands has followed a two-step procedure: in order to identify the component bands, the second derivative has been evaluated as a pre-analysis providing the frequency values and limiting the arbitrary choice of the parameters for the band deconvolution (by using three different software: OPUS 7.5, GRAMS/AI and Origin 8.0). As a representative example, the results of the deconvolution procedure are shown in Figures 6b and 10b.

Infrared spectroscopy is non-invasive methods allowing to get valuable information about the molecular vibrational behavior and then the conformational properties of a large range of systems. In the last years, this technique is more and more used for investigating complex biological systems both in vitro and in vivo. By focusing on the functional groups and chemical bonds which affect to a large extent the biological functions and activity, a detailed picture on proteins, lipids, membranes, cells and tissues can be obtained (Yoshida and Koike 2011; Lewis and McElhaney

2013; Wallach 1972; Lewis and McElhaney 1998; Tamm and Tatulian 1997; Gautier et al 2013; Davis and Mauer 2010; Binder 2007; Naumann et al. 1991; Naumann 2000; Oberreuter et al. 2002). In the peak assignment and in the data interpretation, significant literature on lipids and bacteria has been analyzed (Yoshida and Koike 2011; Lewis and McElhaney 2013; Wallach 1972; Lewis and McElhaney 1998; Tamm and Tatulian 1997; Gautier et al 2013; Davis and Mauer 2010; Binder 2007; Naumann et al. 1991; Naumann 2000; Oberreuter et al. 2002), properly taking into account the significant differences among mycolic acids and other lipids.

3. Results

3.1 FT-IR spectra of single mycolates

Let us start with the analysis of the FT-IR spectra of each mycolate separately, i.e. TMM, TDM and GMM, as shown in Figure 5 and summarized in Table 1.

At a first observation it appears that the 2800-3500 cm^{-1} region is very similar in all the FT-IR mycolate spectra (Figure 5), the only but significant difference being the frequency position of the two main bands; while in the low frequency region, although three main spectral contributions can be identified with several differences in both intensity and width of the specific peaks, and the profile of TMM shows some spectral features which makes it quite different from the two other ones.

The detailed analysis of the different spectral regions allows to assign the vibrational modes to the observed spectral features and to point out the differences among the investigated mycolates.

3.1.1 2800-3500 cm^{-1} region

In the 2800-3500 cm^{-1} region two peaks related to the CH_2 asymmetric and symmetric stretching modes are usually found in lipid spectra around 2920 cm^{-1} and 2850 cm^{-1}, respectively. In our case, in the 2800-2980 cm^{-1} range of the FT-IR spectra (see Figure 6a) of TMM and TDM spectra, these

peaks have the same frequency position, i.e. 2920 cm^{-1} and 2851 cm^{-1} and the same bandwidth, i.e. 20 cm^{-1} and 11 cm^{-1}. The GMM spectrum shows these two peaks at lower frequency, i.e. at 2912 cm^{-1} and 2850 cm^{-1} with smaller bandwidths, i.e. 13 cm^{-1} and 8 cm^{-1}.

In the FT-IR spectra we can observe the presence of two small shoulders in the mycolate spectra, which are related to the CH_3 asymmetric and symmetric stretching vibrations and that are found at 2955 cm^{-1} and 2870 cm^{-1} for TMM, at 2953 cm^{-1} and 2870 cm^{-1} for TDM and at 2954 cm^{-1} and 2871 cm^{-1} for GMM, respectively. It is interesting to observe that the CH_3 asymmetric stretching shoulder is slightly less marked in the TDM spectrum than in the TMM and GMM ones, this latter showing a more distinguishable peak.

Fig. 6b shows a large band reflecting the OH stretching modes centered at 3310 cm^{-1} and 3333 cm^{-1} in the TMM and TDM FT-IR spectrum, respectively, while the GMM FT-IR spectral region is characterized by a structured bump composed by a narrow peak centered at 3316 cm^{-1}, a narrow peak centered at 3426 cm^{-1} and a shoulder at 3204 cm^{-1}.

3.1.2 1215-1800 cm^{-1} region

The comparison among the FT-IR mycolate spectra in the 1215-1800 cm^{-1} region, as shown in Figure 7, points out a significant difference between TMM and TDM, this latter sharing with GMM the four main spectral features, at least in terms of a general shape.

More specifically, in the intermediate FT-IR spectral region two main bands can be identified: the first one at ~1720 cm^{-1} which corresponds to the C=O stretching modes and the second one at ~1470 cm^{-1} which reflects the CH_2 scissoring modes.

The high frequency contribution is centered at 1719 cm^{-1} in the TMM spectrum, at 1724 cm^{-1} in the TDM spectrum and at 1718 cm^{-1} in the GMM spectrum; the bandwidth has the value of 25 cm^{-1}, 34 cm^{-1} and 8 cm^{-1} for TMM, TDM and GMM, respectively, pointing out a very narrow peak in the GMM spectrum.

The contribution at low frequency in the FT-IR TMM spectrum presents a large band covering the 1215-1600 cm^{-1} range, while it is characterized by a series of three main bands in the TDM spectrum.

The frequency analysis of the TDM FT-IR spectrum points out that the first of these bands is identified in the 1400-1470 cm^{-1} range with a predominant narrow peak at 1466 cm^{-1}, the second one in the 1315-1400 cm^{-1} range with a predominant narrow peak at 1377 cm^{-1} (and three shoulders at 1368 cm^{-1}, 1355 cm^{-1} and 1339 cm^{-1}) and in the 1220-1315 cm^{-1} range with a predominant peak at 1278 cm^{-1}, allowing to assign these vibrational contributions to the CH_2 scissoring modes, the CH_3 symmetric and asymmetric bending modes and the CH_2 wagging and twisting modes, respectively. In the GMM spectrum the CH_2 scissoring mode peak is found at 1471 cm^{-1}, followed by a series of a small and narrow peaks with a small bump in the 1320-1430 cm^{-1} range, the highest of these peaks being centered at 1367 cm^{-1}.

On the other hand, in the FT-IR spectra of TMM a small and unstructured band is found in the 1600-1685 cm^{-1} range (where in the other two spectra just a very small shoulder is present) which is centered at 1643 cm^{-1}; the large band covering the 1240-1585 cm^{-1} range is composed by two main contributions, both related to the CH_2 scissoring modes, centered at 1462 cm^{-1} and at 1413 cm^{-1}; a small shoulder is also visible at 1271 cm^{-1} and reflects the CH_2 wagging and twisting modes.

3.1.3 400-1215 cm^{-1} region

The analysis of the 400-1215 cm^{-1} region (see Figure 8) reveals that the three investigated mycolates present a very large band covering the 960-1210 cm^{-1} range, the trehalose mycolates showing a very similar profile.

By analyzing the vibrational features observed in such region of the FT-IR mycolate spectra, one observes that the series of peaks related to the C-O asymmetric and symmetric stretching modes are easily identified in the three mycolate spectra, TMM showing a smaller number of peaks and GMM being characterized by a quite intense and narrow peak attributed to the C-O symmetric stretching modes at 1055 cm^{-1}. In this region the C-O-C bridging band and non-bridging modes of

carbohydrates can be identified around 1150 cm^{-1} and 1080 cm^{-1}, respectively; furthermore, the peak found around 1040 cm^{-1} can be related to the C-OH bending modes of carbohydrates (Davis and Mauer 2010; Naumann et al. 1991; Naumann 2000; Oberreuter et al. 2002).

The C-C stretching modes are reflected in the narrow peak present in the FT-IR spectra of mycolates at 989 cm^{-1} in the TMM spectrum, at 992 cm^{-1} in the TDM spectrum and at 1007 cm^{-1} in the GMM spectrum, pointing out a significant upshift of ~17 cm^{-1} passing from the trehalose mycolates to GMM.

In the TMM spectrum another spectral contribution is identified in the 830-960 cm^{-1} range, characterized by two main peaks centered at 942 cm^{-1} and at 864 cm^{-1} that can be attributed to the combined C-C stretching and C-H rocking modes; in the TDM spectrum these peaks are present at 945 cm^{-1} and at 845 cm^{-1} but they are much less intense than in the TMM spectrum; in the GMM spectrum they are not present.

The analysis among the FT-IR spectra in the higher frequency part of the “fingerprint” region as defined in FT-IR spectra of bacteria since it is characterized by unique features of specific bacteria (Davis and Mauer 2010), shown in Fig. 8b, reveals a narrow peak is present at 805 cm^{-1} and 806 cm^{-1} in the TMM and in the TDM spectrum, respectively. The peak reflecting the CH_2 rocking modes is found at 722 cm^{-1} and 721 cm^{-1} in the TMM and in the TDM spectrum, respectively; while in the GMM spectrum this peak is very intense and downshifted at 713 cm^{-1}.

3.2 FT-IR spectra of mycolate mixtures

Because trehalose mycolates are found in the native mycomembrane as a mixture between TMM and TDM of various chain length and degree of unsaturation, we investigated by FT-IR spectroscopy a mix of TMM/TDM either chemically synthesized or purified from Corynebacterial cells and also a chemically synthesized mixture of TMM/GMM. In Figure 9 the FT-IR spectra of these mixtures are shown and the mode assignment is reported in Table 1, while Figure 13 shows the difference spectrum obtained by subtracting the synthesized TMM/TDM spectrum from the

extracted TMM/TDM spectrum. The above described FT-IR spectra of single mycolates allow us to unambiguously complete the peak assignment of the vibrational features of the extracted TMM-TDM, synthesized TMM-TDM and TMM-GMM.

From a first inspection of the FT-IR spectra (Figure 9), it emerges that the three investigated mycolate mixtures share analogous spectral features at high frequency whereas between 4000 cm^{-1} and 1800 cm^{-1} their spectral profiles have a quite different aspect. By taking into account the single mycolate spectra, one can recognize in the extracted and synthesized TMM-TDM spectra almost all the spectral features found in the TDM spectrum, with the differences due to the presence of additional vibrational contribution in the extracted TMM-TDM spectrum and to the more evident TMM influence in the synthesized TMM-TDM spectrum; on the other hand, the TMM-GMM spectrum points out a vibrational behavior which presents some analogies with the GMM one, but it is affected by the TMM-GMM interaction.

In order to point out the above cited similarities and differences, let us take into account different spectral ranges.

3.2.1 2800-3500 cm^{-1} region

As above described, the 2800-2980 cm^{-1} frequency range of the FT-IR spectra, shown in Figure 10a, is characterized by the presence of the CH_2 asymmetric and symmetric stretching mode peaks, which are identified at 2922 cm^{-1} and 2854 cm^{-1} in the extracted TMM-TDM spectrum, at 2920 cm^{-1} and 2852 cm^{-1} in the synthesized TMM-TDM spectrum and at 2913 cm^{-1} and 2850 cm^{-1} in the TMM-GMM spectrum.

It can be noticed that the obtained frequency values of the CH_2 asymmetric stretching modes are comparable for all the mycolate mixtures, while the CH_2 symmetric stretching modes are characterized by a lower frequency in TMM-GMM than in the TMM-TDM spectra. In addition, the bandwidths of the asymmetric and symmetric CH_2 stretching modes have the values of 14 cm^{-1}, 16 cm^{-1} and 12 cm^{-1} and the values of 8 cm^{-1}, 10 cm^{-1} and 7 cm^{-1}, respectively, for the extracted TMM-TDM, the synthesized TMM-TDM and the TMM-GMM spectrum.

In line with what observed in the single mycolate FT-IR spectra, even in the mycolate mixture FT-IR spectra the two shoulders at higher frequency in respect to the two intense peaks are present: their frequency values are 2954 cm^{-1} and 2871 cm^{-1} for the extracted TMM-TDM spectrum, 2953 cm^{-1} and 2871 cm^{-1} for synthesized TMM-TDM spectrum and 2955 cm^{-1} and 2872 cm^{-1} for the TMM-GMM spectrum, respectively.

We can observe that, although quite influenced by the interaction with TMM, the spectral features are maintained in the TMM-GMM mixture.

Analogously to the case of single mycolates, a quite unstructured large band is also identified in the 3000-3500 cm^{-1} region of the FT-IR spectra of the mycolate mixtures, as reported in Fig. 10b. The synthesized TMM-TDM spectrum is very similar in shape and frequency (3331 cm^{-1}) to the TDM spectrum; in the extracted TMM-TDM and TMM-GMM spectra the band seems to be composed by two peaks, in the first case being centered at 3290 cm^{-1} and 3333 cm^{-1} and in the second case being centered at 3319 cm^{-1} and 3395 cm^{-1} with a shoulder at 3231 cm^{-1}.

3.2.2 1215-1800 cm^{-1} region

Figure 11 shows the 1215-1800 cm^{-1} spectral range of mycolate mixtures. Before analyzing in detail such region, we can qualitatively observe that two main peaks centered at ~1720 cm^{-1} and ~1460 cm^{-1} are detected in all the investigated mycolate mixtures, with a strong deformation due to two additional peaks in the extracted TMM-TDM spectrum, while the other ranges highlight important differences among all the investigated spectra.

The C=O stretching modes are reflected in the highest frequency peak, which is splitted in two peaks centered at 1731 cm^{-1} and 1711 cm^{-1} in the extracted TMM-TDM spectrum, while it is centered at 1723 cm^{-1} and 1718 cm^{-1} in the synthesized TMM-TDM spectrum and in the TMM-GMM spectrum, respectively.

The peak at lowest frequency, i.e. at 1462 cm^{-1}, 1465 cm^{-1} and 1471 cm^{-1} for extracted TMM-TDM, synthesized TMM-TDM and TMM-GMM spectrum, respectively, related to the CH_2 scissoring

modes, presents two small shoulders at 1456 cm^{-1} and 1440 cm^{-1}, 1456 cm^{-1} and 1442 cm^{-1} and at 1456 cm^{-1} and 1445 cm^{-1}, respectively.

Two minor bands are found at 1377 cm^{-1}, 1376 cm^{-1} and 1369 cm^{-1}, for extracted TMM-TDM, synthesized TMM-TDM and TMM-GMM spectrum, respectively, related to the CH_3 symmetric bending modes, with a shoulder at 1340 cm^{-1}, 1340 cm^{-1} and 1334 cm^{-1}, respectively, related to the CH_2 wagging modes, and at 1279 cm^{-1}, 1273 cm^{-1} and 1285 cm^{-1}, respectively, with a small shoulder at 1262 cm^{-1}, 1263 cm^{-1} and 1263 cm^{-1}, respectively, related to the CH_2 twisting modes. The main difference between the two TMM-TDM mixtures is the presence of two very intense peaks at 1655 cm^{-1} and 1548 cm^{-1} in the extracted TMM-TDM. It is significant to observe that in the GMM the peaks corresponding to CH_2 wagging and twisting modes are not clearly distinguishable.

3.2.3 400-1215 cm^{-1} region

The 400-1215 cm^{-1} region, as shown in Figure 12a, presents a main contribution in all the investigated mycolate mixture spectra with a strong difference between the extracted and synthesized TMM-TDM spectra and the TMM-GMM spectrum.

The C-O asymmetric and symmetric stretching modes are reflected in the peaks identified between 1020-1190 cm^{-1}. These peaks are less distinguishable in the TMM-GMM spectrum than in the trehalose mycolate mixture spectra. The frequency values of these contributions are comparable to those obtained for the single mycolates. Furthermore, the upshift observed in the C-C stretching mode peak in the GMM spectrum is still maintained in the TMM-GMM spectrum, where it is composed by two distinguishable contributions. The combined C-C stretching and C-H rocking modes can be referred to the peaks found in the 835 cm^{-1} - 945 cm^{-1} range which are more clearly assigned in the extracted TMM-TDM spectrum.

The “fingerprint” region of the mycolate mixture spectra is shown in Fig. 12b. It shows the narrow peak at 806 cm^{-1}, 806 cm^{-1} and 804 cm^{-1} in the extracted TMM-TDM spectrum, in the synthesized TMM-TDM spectrum and in the TMM-GMM spectrum, respectively. The CH_2 rocking mode peak

seems to be splitted in two components in the extracted TMM-TDM spectrum, centered at 722 cm^{-1} and 700 cm^{-1} due to the presence of additional spectral contributions, while it is a comparable form, intensity and frequency, i.e. 720 cm^{-1} and 714 cm^{-1}, in the synthesized TMM-TDM spectrum and in the TMM-GMM spectrum, respectively to those determined in the single mycolate spectra.

4. Discussion

4.1 2800-3500 cm^{-1} region

By focusing on the 2800-3500 cm^{-1} range of FT-IR spectra of single mycolates, we note that the downshift observed going from trehalose mycolates to the glucose mycolate suggests that the CH_2 asymmetric stretching modes are much slower when the chain is bonded to glucose than when it is bonded to trehalose, that implies a lower freedom of the CH_2 group out from the mycolate chain plane; on the other hand, the frequency of the symmetric stretching modes of this group in GMM is comparable to that observed in TMM and TDM, suggesting that the CH_2 stretching vibrations in the chain plane are similar in all the mycolates. This latter evidence can be linked to the membrane fluidity, since it has been shown that the CH_2 symmetric stretching modes shifts to lower or higher frequency if membranes become harder (or ordered) or softer (or disordered), respectively [Yoshida and Koike 2011; Snyder et al. 1982; Snyder et al. 1996; Fidorra et al. 2006), as a consequence of a decrease or increase of the interaction strength and chain packing. The comparable frequency values of these modes in all the mycolates argue for a comparable lipid fluidity and chain packing; however, the bandwidth values of both the asymmetric and symmetric CH_2 stretching modes seems to point out a slightly higher chain packing in the glucose mycolate compared to the trehalose ones. This latter conclusion finds a confirmation in the comparable values obtained for the CH_2 asymmetric stretching mode frequency in the investigated mycolates and in lipids transiting by an ordered gel phase to a disordered liquid-crystalline phase (Tamm and Tatulian 1997; Cameron et al. 1980; Mendelsohn and Mantsch1986). In addition, the shift observed comparing the two TMM-

TDM mixture spectra can be interpreted as the result of the presence of the –CO-NH-peptide modes in the extracted TMM-TDM mixture, as more clearly pointed out in the 1215-1800 cm^{-1} region (Figure 13).

In line with the results showing that a shift to higher frequency is revealed in the conformational disordering of an all-trans polymethylene chain in dimyristoylphosphatidylserine dispersed in a D_2O-based aqueous buffer (Lewis and McElhaney 2013), with a consequent hydrocarbon chain conformational disorder increase associated to a gauche rotamer formation and all-trans rotamer number decrease (Snyder 1967), we can conclude that TMM and TDM are characterized by the presence of gauche rotamers, while the two rotamer forms, i.e. trans and gauche, coexist in GMM, such difference also influencing the fluidity degree (Liu et al. 1996; Minnikin and Goodfellow 1980; Brennan 1989). This conclusion implies that chains in trehalose mycolates are as packed as in liquid crystalline phase of more extensively investigated lipids (Yoshida and Koike 2011), while they are slightly more tightly packed in glucose mycolate. This evidence is interesting, since membranes are usually found in gel phase at temperature values lower than the melting temperature (Yoshida and Koike 2011), therefore trehalose mycolates show an intrinsically liquid crystalline-like nature.

Another inference can be carried out about localization of trehalose mycolates in the mycomembrane, since disordered phases usually characterize membrane regions of high curvature (Baumgart and Webb 2003), therefore the disordered character of trehalose mycolates suggests that they can be concentrated in high curvature mycomembrane areas.

By analyzing the FT-IR spectra of mycolate mixtures, the downshift above observed for the CH_2 asymmetric stretching mode peaks comparing single trehalose mycolates and glucose mycolate is still maintained when these mycolates are mixed. In addition, the chain packing of the synthesized TMM-TDM mixture is lower than the extracted one, the TMM-GMM mixture showing the highest one. On the other hand, by comparing the bandwidth values of both the CH_2 asymmetric and symmetric stretching modes of single trehalose mycolate and trehalose mycolate mixture FT-IR

spectra, it emerges that the chain packing is higher in the mixtures than in the single mycolates, while the chain packing imposed by GMM is still maintained when it interacts with TMM.

The evidences emerging from the analysis of the CH_3 asymmetric and symmetric stretching modes in single mycolates and mycolate mixtures imply that the stretching modes of this functional group are independent on their number, if one takes into account that in TDM the CH_3 groups are twice than in the monomycolates. It is furthermore possible to conclude that trehalose and glucose show a comparable capability to affect the CH_3 vibrational dynamics.

The difference between the 3000-3500 cm^{-1} region of trehalose and glucose mycolates, shown in Fig. 6b, perfectly reflects the difference observed between the trehalose and the glucose FT-IR spectra in the same regions (Marquez et al. 2018; Wells and Atalla 1990). An inspection of Fig. 10b this spectral region of the mycolate mixtures confirms the strong influence of TDM on the synthesized TMM-TDM mixture and on the extracted TMM-TDM mixture, this latter showing a deformation due to the presence of proteins (that is shown in Figure 13 and will be discussed in the following); the glucose and then GMM features are evident in this spectral region even in the TMM-GMM spectrum.

The effect of the lipophilic environment due to carbon chain can be estimated by the determination of the ratios between the intensities of CH_3 and CH_2 symmetric modes, between the intensities of the CH_2 symmetric modes and the Amide I mode and between the intensities of the CH_2 symmetric modes and the Amide II mode (Grdadolnik 2002; Jiang et al. 2004; Gautier et al 2013; Lewis and McElhaney 2013). The CH_3/CH_2 symmetric mode ratio has the values of 0.37, 0.32 and 0.24 (standard deviation: ±0.02) for TMM, TDM and GMM and the values of 0.38, 0.34 and 0.29 (standard deviation: ±0.02) for the extracted TMM-TDM mixture, the synthesized TMM-TDM mixture and the TMM-GMM mixture. Since this ratio is a measure of the chain order, the decreasing value in the two investigated classes of systems suggests that the chain order decreases following the TMM-TDM-GMM sequence and the extracted TMM-TDM-synthesized TMM-TDM-TMM-GMM; interestingly, the chain order of the mycolate mixtures is increased compared to the single mycolates.

4.2 1215-1800 cm^{-1} region

In the 1215-1800 cm^{-1} region of the TMM and GMM FT-IR spectra, the high frequency band has a vibrational behavior revealing: i) a higher intensity in respect to the low frequency spectral contribution in the GMM spectrum, allowing to conclude that the C=O stretching modes are influenced to the presence of glucose; ii) a higher bandwidth for TDM than for TMM, reflecting the higher number of C=O groups in TDM; iii) the presence of a very narrow peak in the GMM spectrum, emphasizing the more ordered structure imposed by glucose; iv) a slightly lower frequency of the C=O stretching modes in GMM in respect to TMM and especially to TDM, suggesting that these modes are slightly more prevented in the glucose mycolate than in the other ones and hence that they are affected by the glucose presence; v) a higher frequency of the C=O stretching modes in TDM in respect to TMM and GMM and a higher bandwidth in the TDM spectrum as compared to the TMM and GMM spectra, confirming that the double chain of this mycolate and the hydrogen bonded network in TDM strongly affect the C=O vibrations.

By the analysis of the low frequency contribution in this FT-IR spectral region, a more featured profile characterized by the presence of a series of peaks in the TDM spectrum, which are not detected in the other mycolate spectra, is highlighted. This can be the signature of the more ordered nature of TDM. This conclusion is coherent with literature FT-IR data on lipid ordered phases showing in this spectral range a series of peaks reflecting the progression of the CH_2 wagging and twisting modes, which are not observed in phases characterized by a higher chain conformational disorder (Chia and Mendelsohn 1992; Snyder et al. 1996).

In line with these findings, since the most relevant peak of the CH_2 scissoring mode contribution is shifted to higher frequency values in the GMM FT-IR spectrum, we can conclude that the presence of trehalose has the effect to induce a higher order to TMM.

In this FT-IR spectral range of the mycolate mixtures, it is possible to point out very interesting features. The similarity between the TMM-TDM spectral profiles and the TDM one suggests that the vibrational features present in this spectral region are triggered by TDM, whose vibrational

behavior is particularly recognizable in the synthetized TMM-TDM spectrum. In the lower frequency range of this spectral region the peaks found in the TDM spectrum are present in the mixtures, pointing out that the double chain vibrational behavior is predominant in respect to the other contributions.

The splitting of the C=O stretching mode peak is a signature of the effect of both the TMM-TDM interaction, the TDM hydrogen-bonded network and the presence of the protein(s), which is discussed in more detail in the following. More specifically, since the C=O stretching band is splitted in two components in bilayers of hydrated mixed chain phosphatidylserines (Bach and Miller 2001), it is possible to conclude that the extracted TMM-TDM mixture has a behavior comparable to hydrated lipids in respect to the other mycolate mixtures.

The frequency values obtained for the C=O stretching modes are comparable for all the investigated mixtures, while the CH_2 scissoring modes point out an upshift for GMM, where the contributions related to the CH_3 symmetric bending modes are absent; the CH_2 wagging and twisting modes are much faster in the TMM-GMM spectrum. Furthermore, the comparison with the TMM, TDM and GMM FT-IR spectra allows to conclude that their frequency values are maintained in the mixtures even after the interaction between the single mycolates.

An intriguing evidence is pointed out in the higher frequency range of this region of the extracted TMM-TDM FT-IR spectrum pointed out also by the difference spectrum shown in Figure 13: it is very similar to the TDM one except for the two peaks found at 1655 cm^{-1} and 1548 cm^{-1}, which are a clear signature of the presence of a (or more) membrane protein(s), since these frequency values correspond to the amide I and to amide II contributions, respectively, of an α-helical conformation. The value obtained for the α-helical amide I bandwidth is 17 cm^{-1}, which is usually associated to a very stable protein conformation characterized by an α helix-coil transition free energy of more than 300 cal/mole (Chirgadze and Nevskaya 1976). In addition, the presence of the peak reflecting the protein amide III contribution, as shown in Figure 13, can be found in the 1230-1300 cm^{-1}, that overlap with the CH_2 wagging band progression modes (Tamm and Tatulian 1997; Wallach 1972). In the case of the extracted TMM-TDM mixture, the ratio between the CH_2 symmetric modes and

the Amide I mode and between the intensities of the CH_2 symmetric modes and the Amide II mode can be also evaluated, providing the values of 0.85 and 1.66 (standard deviation: ±0.05), respectively (Grdadolnik 2002; Jiang et al. 2004; Gautier et al 2013; Lewis and McElhaney 2013).

By comparing the extracted and synthesized TMM-TDM spectra, it emerges that this (or these) protein(s) could contribute to the lower rigidity of the extracted mycolate mixture, in line with literature data showing that topologically smooth hydrophobic model transmembrane model peptides and surface binding proteins can increase or decrease, respectively, the conformational order in phospholipid bilayers (Lewis and McElhaney 1998; Tamm and Tatulian 1997).

4.3 400-1215 cm^{-1} region

A detailed inspection of the 400-1215 cm^{-1} region of the single mycolate spectra highlights a quite similar profile for TMM and TDM, which is characterized by the C-C stretching mode peak, this spectral feature being more marked and strongly shifted to high frequency in the GMM spectrum; in addition, the large band in the GMM spectrum is less structured than in the other mycolate spectra. These evidences suggest that the C-C and C-O stretching modes are faster in GMM and allow to get a confirmation about the ordering role of the chain by trehalose, while the band related to the CH_2 rocking modes confirm the information about the chain length.

In addition, the spectral analysis of the 400-1215 cm^{-1} region assigns to the C-C stretching modes of TMM and TDM a gauche conformation, whereas these modes in GMM are found in a random arrangement (Wu et al. 2011); as a general conclusion, all the mycolates show a disordered fluid-like nature, since the ordered trans conformations as found in solid lipid phase (Wu et al. 2011) are characterized by a lower vibrational frequency. This evidence is also confirmed by literature findings highlighting that gel-state polymorphism can occur quite often in pure synthesized lipids and very rarely in extracted lipids (Lewis and McElhaney 2013).

The comparison among the FT-IR 400-1215 cm^{-1} region of extracted and synthesized TMM-TDM and TMM-GMM points out a more smoothed profile for this latter mixture. In this region, some spectral contributions in the 600-700 cm^{-1} range of the extracted TMM-TDM spectrum can be

attributed to the N-H bending modes (amide IV and amide V) of the protein(s) (Wallach 1972), as shown in Figure 13. Again, the strong similarity between the extracted TMM-TDM and TDM is reflected not only in the spectral profile, but also in the frequency values of the relevant peaks, which are maintained in all the mixture spectra. It is relevant to point out that the circumstance that the mycolic acids obtained by *C. glutamicum* contain mycolic acids of different chain length, i.e. mainly C32:0, C26:0, C24:0, C34:1, C35:0 (Yang et al. 2012; Lanéelle et al. 2013), has no effect on the vibrational features of the FT-IR spectra, likely due to the predominant amount of mycolic acids with the same (or a comparable) chain length than the synthesized mycolates.

The spectral range points out also a clear evidence about the C-C stretching modes, whose frequencies suggest that a gauche conformation is adopted by the C-C groups in the trehalose mycolate mixtures, while a random conformation is highlighted in the TMM-GMM spectrum.

The comparison between the very low frequency regions of the single mycolate and mycolate mixture FT-IR spectra, shown in Fig. 8b and Fig. 12b, highlight a comparable frequency for the significant peaks characterizing the fingerprint region of trehalose and glucose.

5. Biological implications

Although membrane fluidity has not the same meaning in all the scientific domains (Espinosa et al. 2011; Edidin 1974), there are many different methods and techniques to determine the membrane fluidity and its changes, such as electron spin resonance and fluorescence probes (Cannon et al. 2003), NMR measurement (Rubenstein et al. 1979); oscillatory rheology (Espinosa et al. 2011), and infrared spectroscopy (Yoshida and Koike 2011; Snyder et al. 1996), this latter providing information about the fluidity changes and on the chain packing extent particularly by the CH_2 stretching mode vibrational behavior (Yoshida and Koike 2011).

In addition, the phase transition temperature is related to the chain length and hence mycobacteria are characterized by high transition temperature, low fluidity and low permeability (Liu et al. 1996). Our data provide a confirmation and a molecular explanation for the fluidity of *Corynebacterium*

membrane, pointing out that significant differences exist in conformations adopted by the different mycolates independently on chain length: these conformational features are strictly linked to fluidity, which is comparable but not the same for the different mycolates and their mixtures. This means that fluidity is not only a direct consequence of mycolate chain length, but it is strongly affected by the mycolate conformational behavior. Furthermore, although the chain length can be the same, the interaction between mycolates differing by their polar moiety can affect the fluidity of mycomembrane, determining the different permeability degree. These results contribute to understand the reason why the lipids of *Corynebacteriales* are specifically derived by from trehalose, that is a unique case among the living beings.

It is known that TDM revealed itself to have relevant granulomatous inflammatory action with a toxicity difference between the Corynebacterial strains, the highest level of toxicity being detected in mycobacteria (Ueda et al. 2001; Bekierkunst 1968; Hamasaki et al. 2000).

However, TDM cannot be considered as a virulence factor (Bloch 1950; Noll et al. 1956; Lederer 1984; Lee et al. 1996; Brennan and Nikaido 1995), since its presence (or a slightly variant form) in Corynebacterium, Rhodococcus and Nocardia points out that this is not associated to virulence. Since the granulomatous inflammatory action has been associated to mycoloyl moiety characterized by long chains, while the carbohydrate moiety, i.e. trehalose or glucose, is supposed to be responsible for the biological activities against the host (Ueda et al. 2001; Yano et al. 1988), our data point out that trehalose is able to trigger the mycolate biological functions and to affect the chain order and packing, with a probable consequence on toxicity and inflammation action.

It has been shown that hydrophobicity (Fujita et al. 2005; Dubnau et a. 2000; Ueda et al. 2001; Barry et al. 1998), carbon chain length and structure of mycolic acids of TDM (Gotoh et al. 1991; Liu et al. 1996) are strictly related to the virulence. It has been also pointed out (Kato 1970) that TMM and TDM exert the same action on host-cell mitochondria, with a reducing damaging effect by TMM as compared to TDM. These evidences can find a molecular explanation by our findings highlighting a very similar vibrational behavior of TMM and TDM together with a higher rigidity for TDM with respect to TMM. It is therefore reasonable to suppose that the toxicity and virulence

levels are strongly affected by the specific mycolate interactions and conformational arrangements. In addition, this latter evidence allows to conclude that the mycolate mixture is not a biphasic mixture, which can occur in multicomponent membranes where the leaflet interaction can induce a demixing effect making the lipid bilayer composed by two monophasic monolayers (Ziblat et al. 2010), with the result that the mixture properties, and then the membrane properties, does not reflect the monolayer ones. In our case, there is no phase separation and therefore we can hypothesize that the strong correlation between the single mycolates composing the mixture deeply influence the overall mycomembrane behavior. It is reasonable to suppose that this capability of mycolates is responsible for the optimization of the chain packing and order essential to maintain the membrane functional properties (Feigenson 2007).

Using an experimental model in which an immobile hydrophobic layer supports a TDM-rich, two-dimensionally fluid leaflet, Harland and co-workers (Harland et al. 2008) aimed to determine the capability of TDM to confer dehydration resistance to the membranes. Their results emphasize the fundamental role of TDM connectivity in membrane preservation, adding that the hydrophobic chains can contribute. Our work demonstrates that the chain order and packing are crucial in determining the TDM behavior and hence the TMM-TDM mixture found in mycomembrane, providing useful details on the specific behavior of each functional group both in trehalose and in the chain, on the interactions occurring between the chains and on the extent of the influence of trehalose on the chain.

Finally, our data highlight interesting similarities and differences between the extracted and synthesized TMM-TDM mixtures. The common spectral features found in the two TMM-TDM spectra provide a confirmation about the validity and usefulness of the synthetic model; furthermore, they point out that the extracted lipids are represented by TMM and TDM, as reported by Marchand et al. (Marchand et al. 2012). On the other hand, the presence of α-helix protein(s) in the extracted TMM-TDM mixture is revealed, suggesting that the detected protein(s) in the extracted mycolates could affect the mycolate arrangement through the torsion of the glycosydic bond and hence influence the membrane rigidity, in line with the results showing that a

conformational selection occurs in lectin-carbohydrate complexes as a result of the preference of the primary binding site for the non-reducing end in the case of α bond, with a torsional effect induced by the disaccharide-lectin interaction which is more relevant in the regions involved in such interaction (Sharma and Vijayan 2011).

6. Conclusions

The overall conclusion of the present investigation is that mycolates arrange themselves in the mycomembrane in a specific way allowing to create an environment where all the components of this complex interface, i.e. the mycomembrane, can find their own arrangements where their dynamics can be suitable to their biological functions. The driver of this mycolate arrangement is TDM, whose structural and dynamical properties strongly affect fluidity, rigidity and permeability of the mycomembrane. Furthermore a strong coupling in the mycolate behavior has been demonstrated by the present findings, providing useful details on the underlying molecular mechanisms on mycolate interaction. In the light of these results, our data can contribute to answer to the fundamental question about the "subtle interplay of interactions between the different lipids that endows such a unique mechanical behavior of biological membranes" (Espinosa et al. 2011; Marguet et al. 2006).

FT-IR measurements have been performed on bacterial cells in order to provide an identification of different strains by the investigation of five main spectral regions, which has been used for food characterization and for creating bacterial databases (Davis and Mauer 2010; Naumann et al. 1991; Naumann 2000; Oberreuter et al. 2002; Filipa et al. 2004; Jiang et al. 2004). The qualitative comparison between the existing spectra of bacterial cells and our data on mycolates extracted from the corynebacterial mycomembrane opens the way for different conclusions: i) the five regions that are usually characterized for the bacterial investigations (Davis and Mauer 2010; Naumann et al. 1991; Naumann 2000; Oberreuter et al. 2002) show vibrational features which are analogous to those observed in our extracted TMM-TDM spectrum, so allowing to conclude that mycolates and

carbohydrates play a key role strongly affecting the whole membrane and bacterial behavior; ii) although a series of isolation and extraction procedures have been applied to obtain the mycolate mixture, the similarity of the bacterial and mycolate mixture spectra and especially the presence of all the significant peaks related to the vibrational modes, whose characterization allows the bacterial identification, represent a validity proof of our approach; iii) the presence of protein traces in our FT-IR mycolate mixture spectrum revealed itself a great advantage, since in the bacterial IR spectra the amide I and amide II contributions often predominate (Davis and Mauer 2010; Filipa et al. 2004) on another relevant vibrational contribution, i.e. the 1720 cm^{-1} peak, so preventing a detailed study of the C=O stretching modes, which provide useful information.

The present work is to be collocated in the framework of a systematic study of corynebacteria by spectroscopic techniques, which provide access to different space and time scales. Moving from simple to complex, the systematic analysis of the FT-IR spectra of each single pure system composing the mycomembrane will allow to clarify how such interaction modifies its original structural and dynamical properties. Due to the power and versatility shown by FT-IR methods, we will apply these techniques to investigate mycolate systems of increasing complexity, including progressively into the mycolate mixtures other membrane components (phospholipids, proteins (in the proper ratio), ...), in order to selectively understand the role of each of them in determining the mycomembrane properties by their mutual interactions.

The final goal will be the study of the bacterial envelope and then of the whole bacterium in order to perform a detailed comparison with monoderm or diderm bacterial spectra and to identify spectra corresponding to the signature of the mycomembrane of Corynebacteriales as compared to the cytoplasmic membrane or the LipoPolySaccharide-containing outer membrane of Gram negative bacteria.

Since our innovative approach allows, as we show in the present paper, to relate the observed vibrational features to the fluidity, rigidity and permeability properties of the whole system, it will lead to a new characterization of corynebacteria and mycobacteria in strong relation with the tuberculosis treatment research.

Acknowledgements

FM acknowledges the Fondation Paris-Saclay for the Jean d'Alembert fellowship 2016-2017 "Multiscale study of the structure of the outer membrane of mycobacteria: from the lipidic composition to the functional properties".

We want to thank Christiane Dietrich for her excellent technical assistance for lipid extraction from *C. glutamicum*.

References

Bach, D., Miller, I.R. 2001. Attenuated total reflection (ATR) Fourier transform infrared spectroscopy of dimyristoyl phosphatidylserine-cholesterol mixtures. Biochimica et Biophysica Acta. 1514, 318-326.

Barry, C. E., 3rd, Lee, R. E., Mdluli, K., Sampson, A. E., Schroeder, B. G., Slayden, R. A., Yuan, Y. 1998. Mycolic acids: structure, biosynthesis and physiological functions. Prog- Lipid Res. 37, 143–179.

Baumgart, H., Webb, W. 2003. Imaging coexisting fluid domains in biomembrane models coupling curvature and line tension. Nature. 425, 821-824.

Bekierkunst, A. 1968Acute granulomatous response produced in mice by trehalose-6,6-dimycolate. J Bacteriol. 96, 958–61.

Beukes, M., Lemmer, Y., Deysel, M., Al Dulayymi, J. R., Baird, M. S., Koza, G., Iglesias, M. M., Rowles, R. R., Theunissen, C., Grooten, J., Toschia, G., Roberts, V. V., Pilcher, L., Van Wyngaardt, S., Mathebula, N., Balogun, M., Stoltz, A. C., Verschoor, J. A. 2010. Structure–function relationships of the antigenicity of mycolic acids in tuberculosis patients, Chem. Phys. Lipids 163, 800–808.

Binder, H. 2007. Water near lipid membranes as seen by infrared spectroscopy. Eur. Biophys. J. 36, 265-279.

Bloch, H. 1950. Studies on the virulence of tubercle bacilli. Isolation and biological properties of a constituent of Granulomatous inflammation and toxicity virulent organisms. J. Exp. Med. 91, 197–218.

Brennan, P. J. 1989. Structure of mycobacteria: recent developments in defining cell wall carbohydrates and proteins. Rev. Infect. Dis. 11, S420-S430.

Brennan, P.J., Nikaido, H. 1995. The envelope of mycobacteria. Annu. Rev. Biochem. 64, 29–63.

Cameron, D. G., Casal, H.L., Mantsch, H.H. 1980. Characterization of the pre-transition in 1,2-dipalmitoyl-sn-glycero-3-phosphocholine by Fourier transform infrared spectroscopy. Biochemistry. 19, 3665-3672.

Cannon, B., Heath, G., Huang, J., Somerharju, P., Virtanen, J.A., Cheng, K.H. 2003. Time-resolved fluorescence and Fourier transform infrared spectroscopic investigations of lateral packing defects and superlattice domains in compositionally uniform cholesterol/phosphatidylcholine bilayers. Biophys. J. 84, 3777–3791.

Chia, N.-C., Mendelsohn, R. 1992. CH_2 wagging modes of unsaturated acyl chains as IR probes of conformational order in methyl alkenoates and phospholipid bilayers, J. Phys. Chem. 96, 10543-10547.

Chirgadze, Y. N., Nevskaya, N. A. 1976. Infrared spectra and resonance interaction of amide-I vibration of the antiparallel-chain pleated sheet. Biopolymers. 15, 607-625.

Davis, R., Mauer, L.J. 2010. Fourier transform infrared (FT-IR) spectroscopy: A rapid tool for detection and analysis of foodborne pathogenic bacteria. In: Current Research, Technology and Education Topics in Applied Microbiology and Microbiological Biotechnology, 1582, Mendez-Vilas, A. (Eds.). Formatex Research Center. pp.1582-1594.

Dubnau, E., Chan, J., Raynaud, C., Mohan, V. P., Lanéelle, M. A., Yu, K., Quemard, A., Smith, I. & Daffé , M. 2000. Oxygenated mycolic acids are necessary for virulence of Mycobacterium tuberculosis in mice. Mol Microbiol. 36, 630–637.

Edidin, M. 1974. Rotational and translational diffusion in membranes. Ann. Rev. Biophys. Bioeng. 3, 179–201.

Espinosa, G., López-Montero, I., Monroy, F., Langevin, D. 2011. Shear rheology of lipid monolayers and insights on membrane fluidity. Proc. Natl. Acad. Sci. USA. 108, 6008–6013.

Feigenson, G.W. 2007. Phase boundaries and biological membranes. Annu. Rev. Biophys. Biomol. Struct. 36, 63–77.

Fidorra, M., Duelund, L., Leidy, C., Simonsen, A.C., Bagatolli, L.A. 2006. Absence of fluid ordered/fluid-disordered phase coexistence in ceramide/POPC mixtures containing cholesterol. Biophys. J. 90, 4437–4451.

Filipa, Z., Herrmann, S., Kubat, J. 2004. FT-IR spectroscopic characteristics of differently cultivated Bacillus subtilis. Microbiol. Res. 159, 257–262.

Fujita, Y., Naka, T., McNeil, M. R., Yano, I. 2005. Intact molecular characterization of cord factor (trehalose 6,69-dimycolate) from nine species of mycobacteria by MALDI-TOF mass spectrometry. Microbiology. 151, 3403–3416.

Gautier, J., Passot, S., Pénicaud, C., Guillemin, H., Cenard, S., Lieben, P., Fonseca, F. A low membrane lipid phase transition temperature is associated with a high cryotolerance of *Lactobacillus delbrueckii* subspecies *bulgaricus* CFL1. 2013. J. Dairy Sci. 96, 591–5602.

Global tuberculosis report 2018. Geneva: World Health Organisation; 2018. License: CC BY-NC-SA 3.0 IGO.

Gotoh, K., Mitsuyama, M., Imaizumi, S., Kawamura, I., Yano, I. 1991. Mycolic acid-containing glycolipid as a possible virulence factor of Rhodococcus equi for mice. Microbiol. Immunol. 35, 175–185.

Hamasaki, N., Isowa, K. I., Kamada, K., Terano, Y., Matsumoto, T., Arakawa, T., Kobayashi, K., Yano, I. 2000. In vivo administration of mycobacterial cord factor (trehalose 6,6′-dimycolate) can induce lung and liver granulomas and thymic atrophy in rabbits. Infect. Immun. 68, 3704–3709.

Harland, C. W., Rabuka, D., Bertozzi, C. R., Parthasarathy, R. 2008. The Mycobacterium tuberculosis Virulence Factor Trehalose Dimycolate Imparts Desiccation Resistance to Model Mycobacterial Membranes. Biophys. J. 94, 4718–4724.

Hsu, F., Soehl, K., Turk, J., Haas, A. 2011. Characterization of mycolic acids from the pathogen Rhodococcus equi by tandem mass spectrometry with electrospray ionization. Anal. Biochem. 409, 112–122.

Hunter, R. L., Venkataprasad, N., Olsen, M. R. 2006. The role of trehalose dimycolate (cord factor) on morphology of virulent M. tuberculosis in vitro. Tuberculosis. 86, 349–356.

Indrigo, J., R. L. Hunter Jr., and J. K. Actor. 2003. Cord factor trehalose 6,69-dimycolate (TDM) mediates trafficking events during mycobacterial infection of murine macrophages. Microbiology. 149, 2049–2059.

Jiang, W., Saxena, A., Song, B., Ward, B. B., Beveridge, T. J., Myneni, S. C. B. 2004. Elucidation of Functional Groups on Gram-Positive and Gram-Negative Bacterial Surfaces Using Infrared Spectroscopy. Langmuir. 20, 11433-11442.

Kai, M., Y. Fujita, Y. Maeda, N. Nakata, S. Izumi, I. Yano, and M. Makino. 2007. Identification of trehalose dimycolate (cord factor) in Mycobacterium leprae. FEBS Lett. 581, 3345–3350.

Kanemaru, M., Yamamoto, K., Kadokawa, J.-I. 2012. Self-assembling Properties of 6-O-Alkyltrehaloses under Aqueous Conditions. Carbohydr. Res. 357, 32-40.

Kato, M. 1970. Site II-specific inhibition of mitochondrial oxidative phosphorylation by trehalose-6, 6'-dimycolate (cord factor) of Mycobacterium tuberculosis. Arch. Biochem. Biophys. 140, 379-390.

Korf, J.E., Stolz, A., Verschoor, J.A., De Baetselier, P., Grooten, J. 2005. The Mycobacterium tuberculosis cell wall component mycolic acid elicits pathogen-associated host innate immune responses. Eur. J. Immunol. 35, 890–900.

Korf, J.E., Pynaert, G., Tournoy, K., Boonefaes, T., Van Oosterhout, A., Ginneberge, D., Haegeman, A., Verschoor, J.A., De Baetselier, P., Grooten, J. 2006. Macrophage reprogramming by

mycolic acid promotes a tolerogenic response in experimental asthma. Am. J. Resp. Crit. Care Med. 174, 152–160.

Kurita, K., Masuda, N., Aibe, S., Murakami, K., Ishii, S., Nishimura, S. 1994. Macromolecules. 27, 7544-7549.

Lanéelle, M.-A., Tropis, M., Daffé, M. 2013. Current knowledge on mycolic acids in Corynebacterium glutamicum and their relevance for biotechnological processes. Appl. Microbiol. Biotechnol. 97, 9923–9930.

Lederer, E. 1984. Chemistry of mycobacterial cord factor and related natural and synthetic trehalose esters. In: Kubica, G.P., Wayne, L.G. (Eds.), The mycobacteria: a sourcebook part A. Marcel Dekker, New York, pp. 361–377.

Lee, R.E., Brennan, P.J., Besra, G.S. 1996. Mycobacterium tuberculosis cell envelope. Curr. Top. Microbiol. Immunol. 215, 1–27.

Lewis, R.N.A.H., McElhaney, R.N. 2013. Membrane lipid phase transitions and phase organization studied by Fourier transform infrared spectroscopy, Biochimica et Biophysica Acta. 1828, 2347–2358.

Liu, J., Barry III, C. E., Besra, G. S., Nikaido, H. 1996. Mycolic Acid Structure Determines the Fluidity of the Mycobacterial Cell Wall. J. Biol. Chem. 271, 29545–29551.

Lu, W., Navidpour, L., Taylor, S. D. 2005. Carbohydr. Res., 340, 1213-1271.

Marchand, C. H., Salmeron, C., Bou Raad, R., Méniche, R., Chami, M., Masi, M., Blanot, D., Daffé, M., Tropis, M., Huc, E., Le Maréchal, P., Decottignies, P., Bayan, N. 2012. Biochemical Disclosure of the Mycolate Outer Membrane of Corynebacterium glutamicum. J. Bacteriol. 194, 587–597.

Marguet, D., Lenne, P.F., Rigneault, H., He, H.T. 2006. Dynamics in the plasma membrane: How to combine fluidity and order. EMBO J. 25, 3446–3457.

Marquez, M. J., Romani, D., Diaz, S. B., Brandan, S. A. 2018. Structural and vibrational characterization of anhydrous and dihydrated species of trehalose based on the FTIR and FTRaman spectra and DFT calculations. J. King Saud University – Science. 30, 229–249.

Mendelsohn, R., Mantsch, H.H. 1986. Fourier transform infrared studies of lipidprotein interaction. In: Watts, A., DePont, J. J. H. H. M. (Eds.), Progress in Protein-Lipid Interactions. Elsevier Science Publishers, Amsterdam, pp. 103-146.

Minnikin, D. E., Goodfellow, M. 1980. Lipid composition in the classification and identification of acid-fast bacteria. In: Goodfellow, M., Board, R. G. (Eds.), Microbiological Classification and Identification, Academic Press, London, pp. 189–256.

Nabeshima, S., Murata, M., Kashiwagi, K., Fujita, M., Furusyo, N., Hayashi, J. 2005. Serum antibody response to tuberculosis-associated glycolipid antigen after BCG vaccination in adults. J. Infect. Chemother. 11, 256–258.

Naumann, D., Helm, D., Labischinski, H. 1991. Microbiological characterizations by FT-IR spectroscopy. Nature. 351, 81-82.

Naumann, D. 2000. Infrared spectroscopy in Microbiology. In: Meyers, R.A. (Eds.). Encyclopedia of Analytical Chemistry. John Wiley and Sons, Chichester, UK. pp. 102-131.

Nishiuchi, Y., Baba, T., Hotta, H.H., Yano, I. 1999. Mycolic acid analysis in Nocardia species: The mycolic acid compositions of Nocardia asteroides, N. farcinica, and N. nova. J. Microbiol. Meth. 37, 111–122.

Noll, H., Bloch, H., Asselineau, J., Lederer, E. 1956. The chemical structure of the cord factor of Mycobacterium tuberculosis. Biochim Biophys Acta. 20, 226–233.

Oberreuter, H. Seiler, H., Scherer, S. 2002. Identification of coryneform bacteria and related taxa by Fourier-transform infrared (FT-IR) spectroscopy. Int. J. System. Evolution. Microbiol. 52, 91–100.

Perrin, D.D., Armarego, W.L.F. 1997. Purification of Laboratory Chemicals. Butterworth-Heinemann (Eds.).

Portevin, D., De Sousa-D'Auria, C., Houssin, C., Grimaldi, C., Chami, M., Daffé, M., Guilhot, C. 2004. A polyketide synthase catalyzes the last condensation step of mycolic acid biosynthesis in mycobacteria and related organisms. Proc. Natl. Acad. Sci. USA. 101, 314–319.

Prandi, J. 2012. A convenient synthesis of glucose monomycolate. Carbohydr. Res. 347, 151-154.

Ratovelomanana-Vidal, V., Girard, C., Touati, R., Tranchier, J. P., Ben Hassine, B., Genêt, J. P. 2003. Enantioselective Hydrogenation of β-Keto Esters using Chiral Diphosphine-Ruthenium Complexes: Optimization for Academic and Industrial Purposes and Synthetic Applications. Adv. Synth. Catal. 345, 261-274.

Rubenstein, J.L.R., Smith, B.A., McConnell, H.M. 1979. Lateral diffusion in binary mixtures of cholesterol and phosphatidylcholines. Proc. Natl. Acad. Sci. USA. 76, 15–18.

Ryll, R., Kumazawa, Y., Yano, I. 2001. Immunological properties of trehalose dimycolate (cord factor) and other mycolic acid-containing glycolipids a review. Microbiol. Immunol. 45, 801–811.

Sekanka, G., Baird, M., Minnikin, D., Grooten, J. 2007. Mycolic acids for the control of tuberculosis. Expert Opin. Ther. Patents 17, 315–331.

Sharma, A., Vijayan, M. 2011. Influence of glycosidic linkage on the nature of carbohydrate binding in β-prism I fold lectins: An X-ray and molecular dynamics investigation on banana lectin–carbohydrate complexes. Glycobiology. 21, 23–33.

Snyder, R.G. 1967. Vibrational study of the chain conformation of the liquid n-paraffins and molten polyethylene. J. Chem. Phys. 47, 1316–1360.

Snyder, R.G., Strauss, H.L., Elliger, C.A. 1982. Carbon-hydrogen stretching modes and the structure of n-alkyl chains. 1. Long, disordered chains, J. Phys. Chem. 86, 5145–5150.

Snyder, R.G., Liang, G.L., Strauss, H.L., Mendelsohn, R. 1996. IR spectroscopic study of the structure and phase behavior of long-chain diacylphosphatidylcholines in the gel state. Biophys. J. 71, 3186–3198.

Spargo, B. J., Crowe, L. M., Ioneda, T., Beaman, B. L., Crowe, J. H. 1991. Cord factor (alpha,alpha-trehalose 6,69-dimycolate) inhibits fusion between phospholipid vesicles. Proc. Natl. Acad. Sci. USA. 88, 737–740.

Tamm, L. K., Tatulian, S. A. 1997. Infrared spectroscopy of proteins and peptides in lipid bilayers. Quarter. Rev. Biophys. 30, 365-429.

Ueda, S., Fujiwara, N., Naka, T., Sakaguchi, I., Ozeki, Y., Yano, I., Kasama, T., Kobayashi, K. 2001. Structure–activity relationship of mycoloyl glycolipids derived from Rhodococcus sp. 4306. Microbial Pathogenesis. 30, 91–99.

Van der Peet. P. L., Gunawan, C., Torigoe, S., Yamasaki, S., Williams, S. J. 2015. Corynomycolic acid-containing glycolipids signal through the pattern recognition receptor Mincle. Chem. Commun. 51, 5100-5103.

Verschoor, J. A., Baird, M. S., Grooten, J. 2012. Towards understanding the functional diversity of cell wall mycolic acids of Mycobacterium tuberculosis, Progr. Lipid Res. 51, 325–339.

Wallach, D. F. H. 1972. Infrared and Laser Raman Spectroscopy in membrane analysis. Che. Phys. Lipids. 8, 347-354.

Wells Jr., H. A., Atalla, R. H. 1990. An investigation of the vibrational spectra of glucose, galactose and mannose. J. Mol. Struct. 224, 385-424.

Wood, R. 2007. Challenges of TB diagnosis and treatment in South Africa. South. Afr. J. HIV Med. 27, 44–48.

Wu, H., Volponi, J. V., Oliver, A. E., Parikh, A. N., Simmons, B. A., Singh, S. 2011. In vivo lipidomics using single-cell Raman spectroscopy, PNAS. 108, 3809–3814.

Yang, Y., Shi, F., Tao, G., Wang, X. 2012. Purification and structural analysis of mycolic acids in Corynebacterium glutamicum. J. Microbiol. 50, 235–240.

Yano, I., Oka, S., Natsuhara, Y., Kato, Y., Tomiyasu, I., Kaneda, K. 1988. Molecular structure and immune-pharmacological activities of the new glycolipids containing mycolic acids in actinomycetales. In: Okami, Y., Beppu, T., Ogawara, H. (Eds.), Japan Scientific Societies Press, Tokyo, pp. 469–477.

Yoshida, S., Koike, K. 2011. Lipid and Membrane Dynamics in Biological Tissues - Infrared Spectroscopic Studies. Advances in Planar Lipid Bilayers and Liposomes. 13, 1-32.

Ziblat, R., Leiserowitz, L., Addadi, L. 2010. Crystalline domain structure and cholesterol crystal nucleation in single hydrated DPPC:cholesterol:POPC bilayers. J. Am. Chem. Soc. 132, 9920–9927.

Figure captions

Figure 1. TMM, TDM and GMM chemical synthesis starting from corynomycolic acid **1**, trehalose derivative **2** and glucose derivative **3**. Bn = benzyl

Figure 2. Corynomycolic acid **1** prepared starting from β-ketoester **4**. Binap = 2,2'-bis(diphenylphosphino)-1,1'-binaphthyl; HMPA = hexamethylphosphoramide; LDA = lithium diisopropylamide; THF = tetrahydrofuran

Figure 3. GMM, TMM and TDM prepared by nucleophilic substitution of tosylate groups of **7**, **8** and **9** using the cesium salt of mycolic acid. Bn = benzyl; DMF = *N*,*N*-dimethylformamide; THF = tetrahydrofuran ; Ts = *para*-toluenesulfonyl

Figure 4. ^{1}H NMR spectra of GMM, TMM and TDM (360MHz, $CDCl_3/CD_3OD$)

Figure 5. FT-IR spectra (500-3500 cm^{-1}) of TMM, TDM and GMM

Figure 6. 2800-3500 cm^{-1} region of FT-IR spectra of TMM, TDM and GMM with the CH_2 asymmetric and symmetric stretching modes and the CH_3 asymmetric and symmetric stretching. In the GMM spectrum in b) the deconvolution result is shown.

Figure 7. 1215-1800 cm^{-1} region of FT-IR spectra of TMM, TDM and GMM with the C=O stretching modes and the CH_2 scissoring modes

Figure 8. 400-1215 cm^{-1} region of FT-IR spectra of TMM, TDM and GMM with the C-O asymmetric and symmetric stretching modes, the C-C stretching modes and the C-H rocking modes

Figure 9. FT-IR spectra (500-3500 cm^{-1}) of chemically synthesized and extracts from Corynebacteria TMM/TDM and chemically synthesized TMM/GMM

Figure 10. 2800-3500 cm^{-1} region of FT-IR spectra of synthesized and extracted TMM/TDM and TMM/GMM with the CH_2 asymmetric and symmetric stretching modes and the CH_3 asymmetric and symmetric stretching. In the TMM/GMM spectrum in b) the deconvolution result is shown.

Figure 11. 1215-1800 cm^{-1} region of FT-IR spectra of FT-IR spectra of synthesized and extracted TMM/TDM and TMM/GMM with the C=O stretching modes and the CH_2 scissoring modes

Figure 12. 400-1215 cm^{-1} region of FT-IR spectra of synthesized and extracted TMM/TDM and TMM/GMM with the C-O asymmetric and symmetric stretching modes, the C-C stretching modes and the C-H rocking modes

Figure 13. Difference spectrum obtained by subtracting the synthesized TMM/TDM spectrum from the extracted TMM/TDM spectrum with the protein spectral contributions

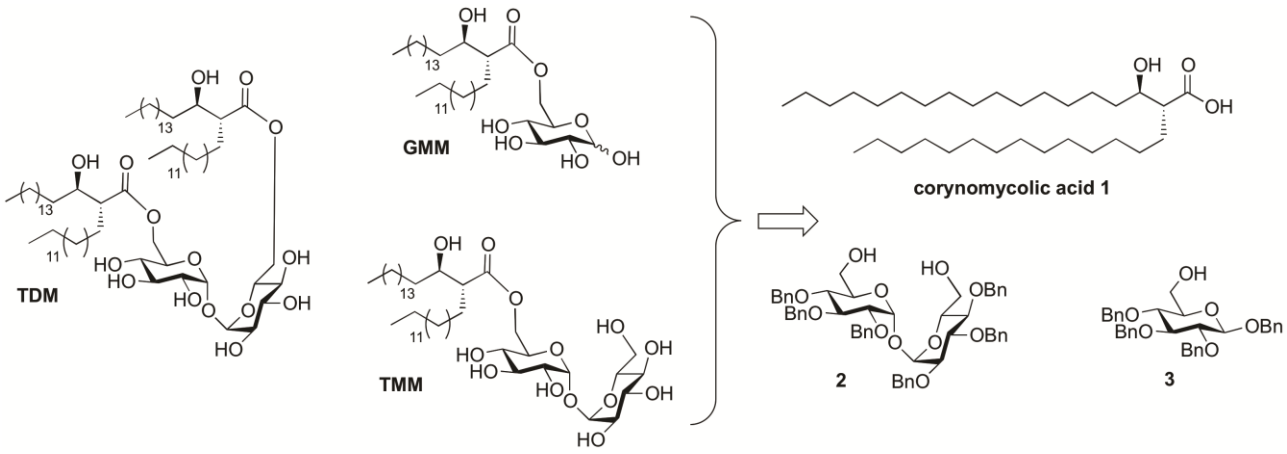

Figure 1. TMM, TDM and GMM chemical synthesis starting from corynomycolic acid **1**, trehalose derivative **2** and glucose derivative **3**. Bn = benzyl

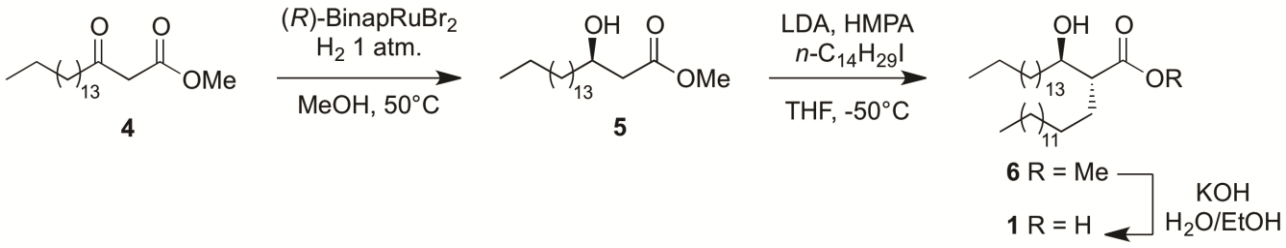

Figure 2. Corynomycolic acid **1** prepared starting from β-ketoester **4**. Binap = 2,2'-bis(diphenylphosphino)-1,1'-binaphthyl; HMPA = hexamethylphosphoramide; LDA = lithium diisopropylamide; THF = tetrahydrofuran

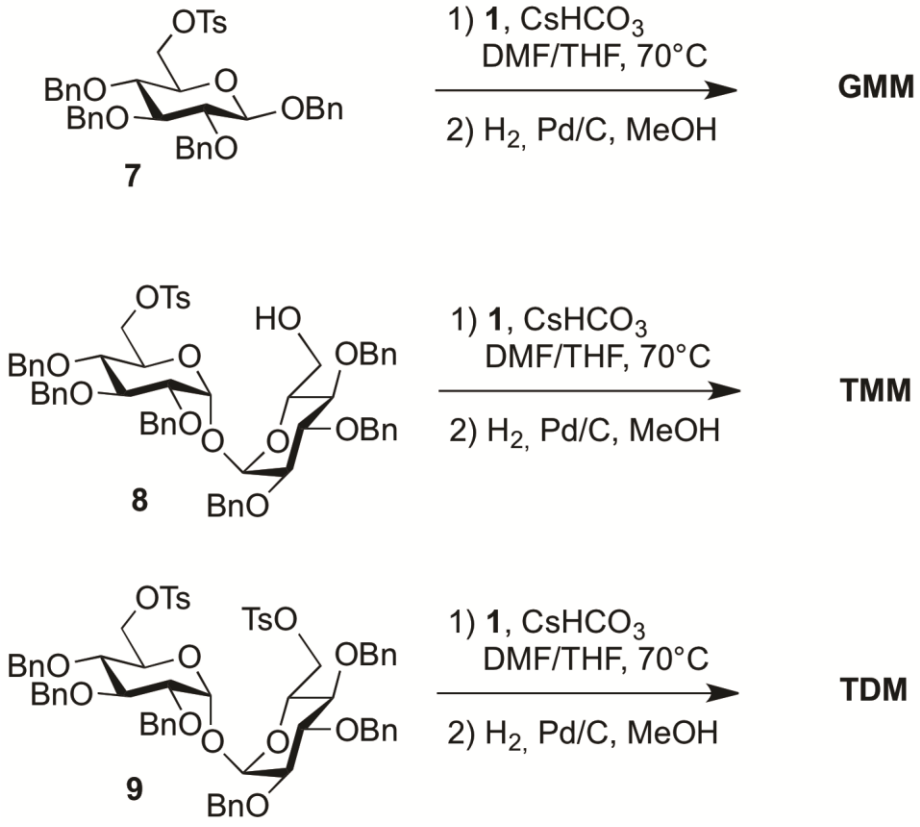

Figure 3. GMM, TMM and TDM prepared by nucleophilic substitution of tosylate groups of **7**, **8** and **9** using the cesium salt of mycolic acid. Bn = benzyl; DMF = *N*,*N*-dimethylformamide; THF = tetrahydrofuran ; Ts = *para*-toluenesulfonyl

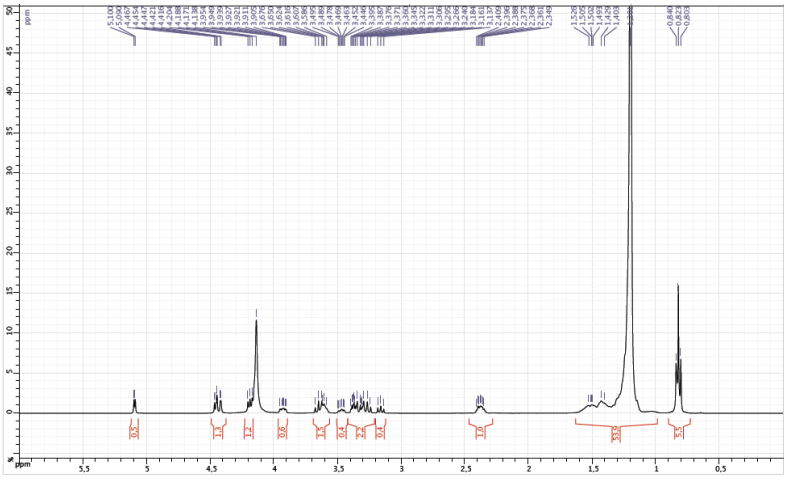
a)

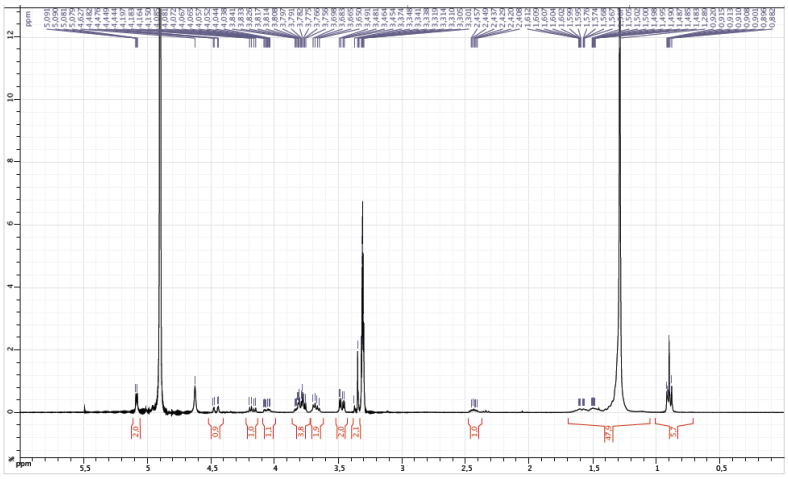
b)

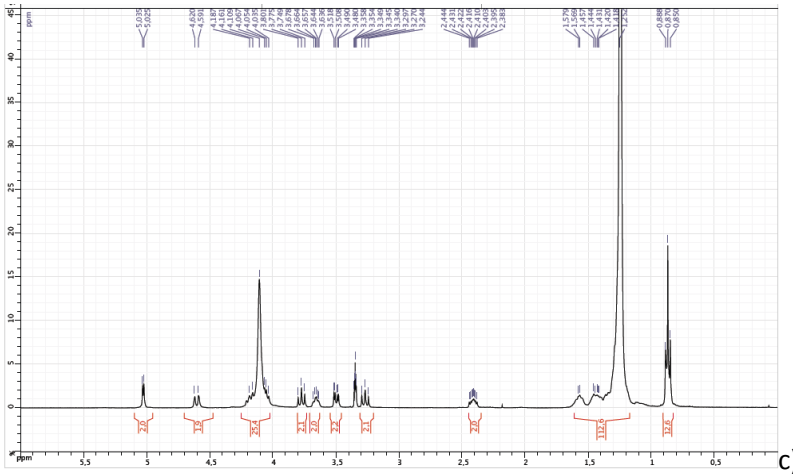
c)

Figure 4. ^{1}H NMR spectra of a) GMM, b) TMM and c) TDM (360MHz, $CDCl_3/CD_3OD$)

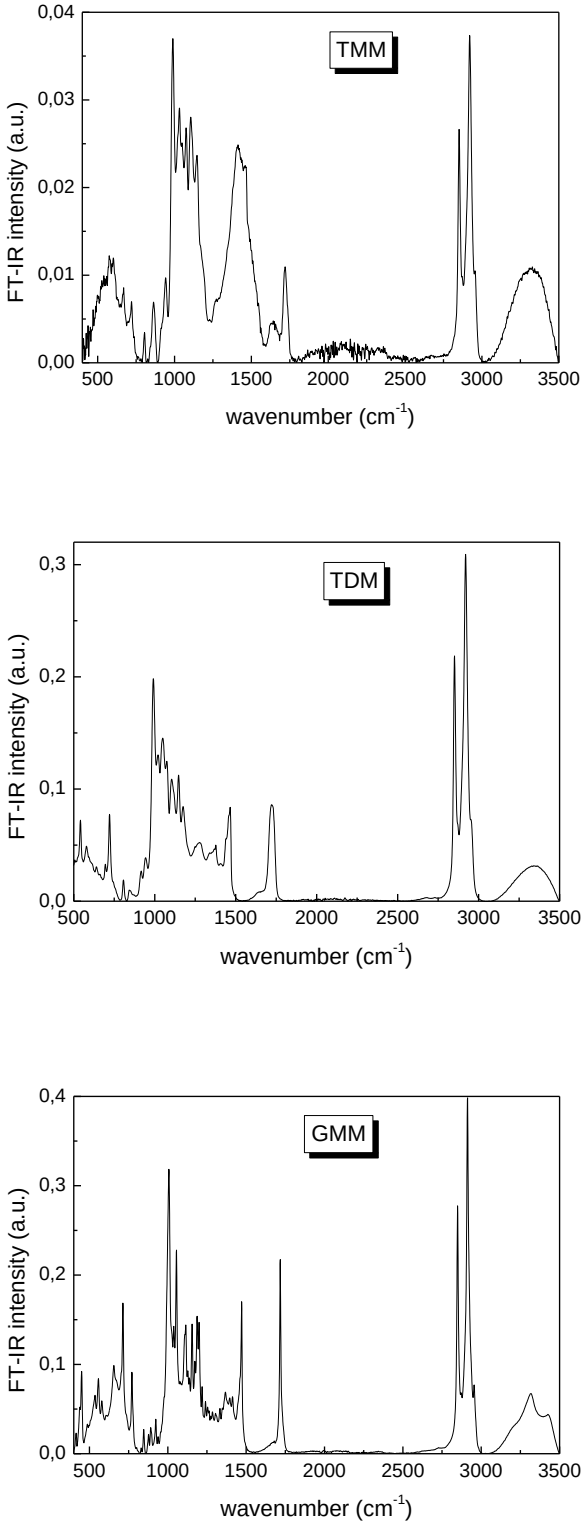

Figure 5. FT-IR spectra (500-3500 cm^{-1}) of TMM, TDM and GMM

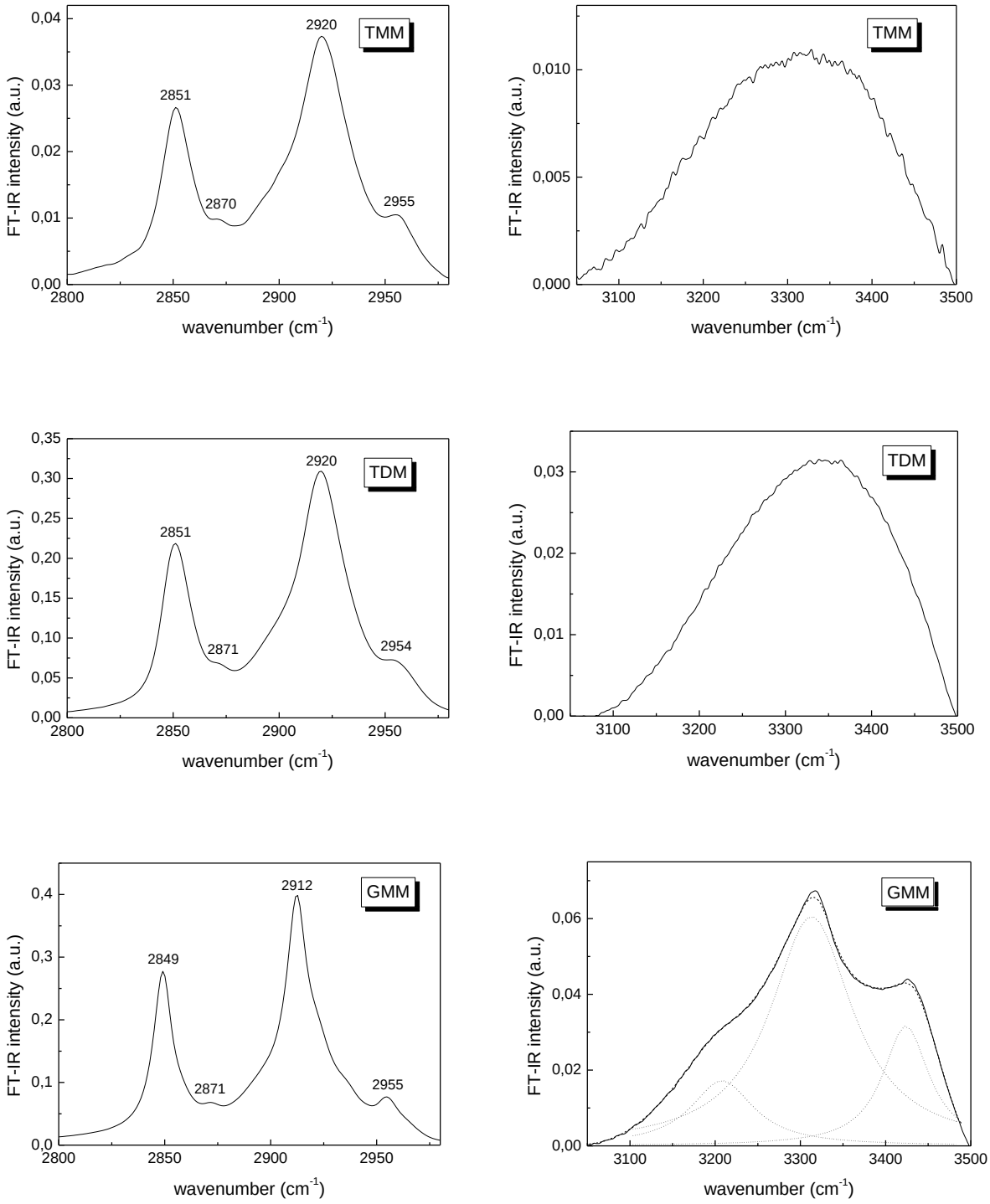

a) b)

Figure 6. 2800-3500 cm^{-1} region of FT-IR spectra of TMM, TDM and GMM with the CH_2 asymmetric and symmetric stretching modes and the CH_3 asymmetric and symmetric stretching. In the GMM spectrum in b) the deconvolution result is shown.

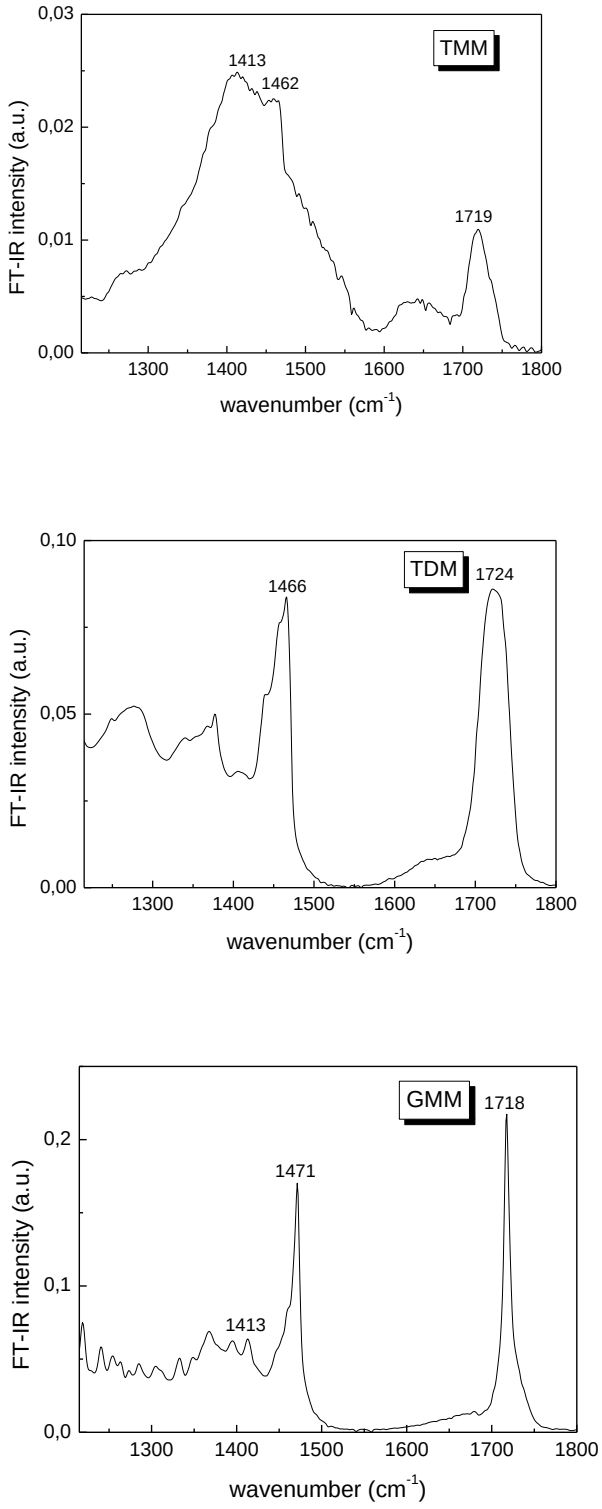

Figure 7. 1215-1800 cm^{-1} region of FT-IR spectra of TMM, TDM and GMM with the C=O stretching modes and the CH_2 scissoring modes

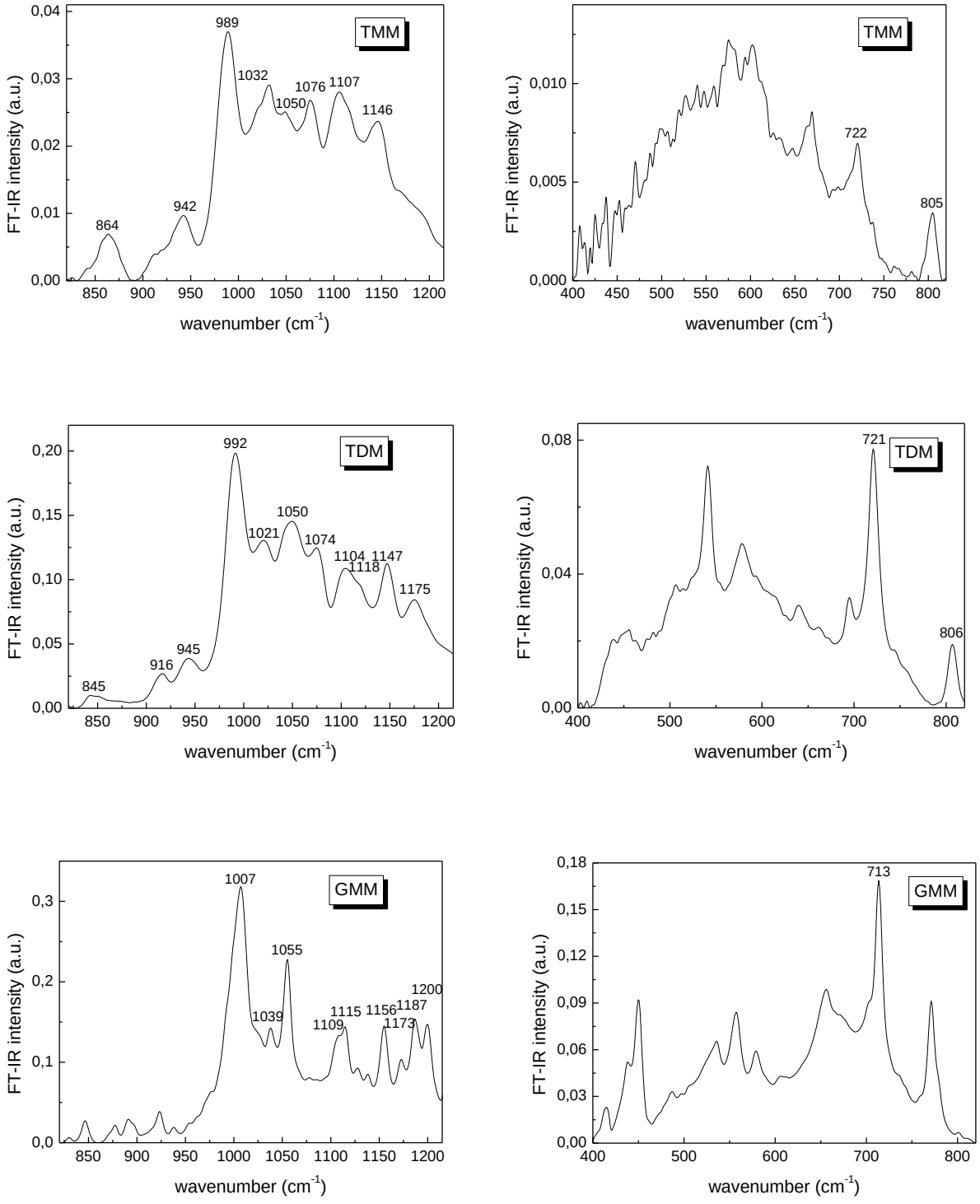

Figure 8. 400-1215 cm^{-1} region of FT-IR spectra of TMM, TDM and GMM with the C-O asymmetric and symmetric stretching modes, the C-C stretching modes and the C-H rocking modes

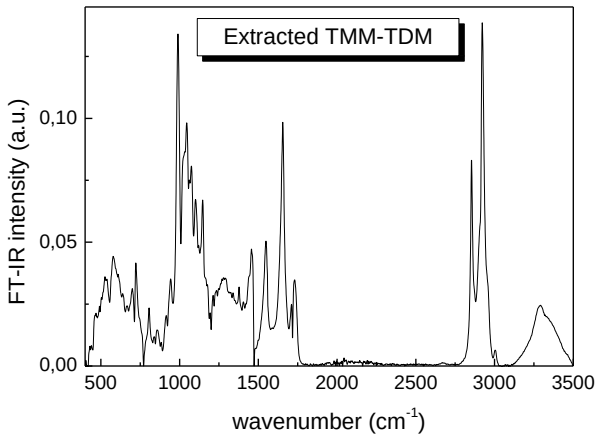

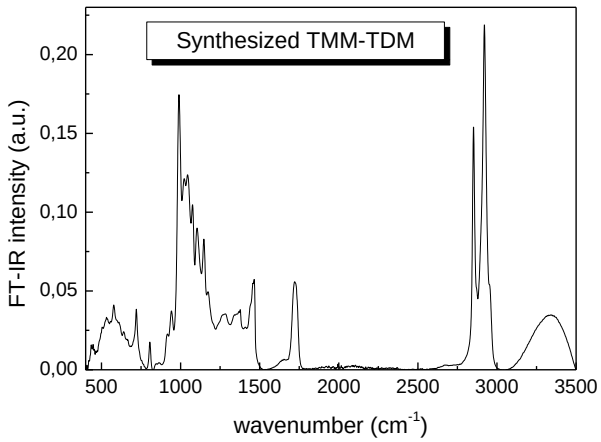

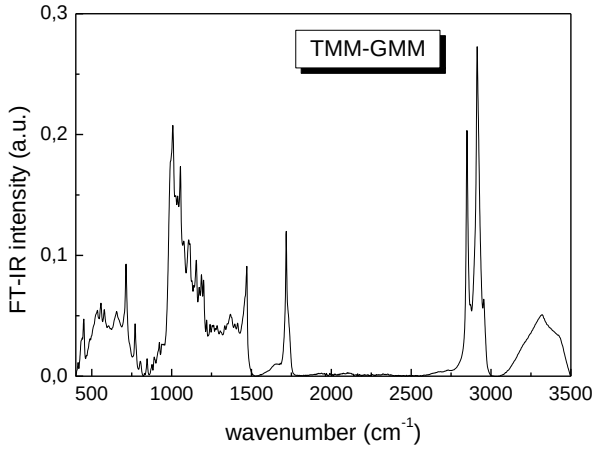

Figure 9. FT-IR spectra (500-3500 cm^{-1}) of chemically synthesized and extracts from Corynebacteria TMM/TDM and chemically synthesized TMM/GMM

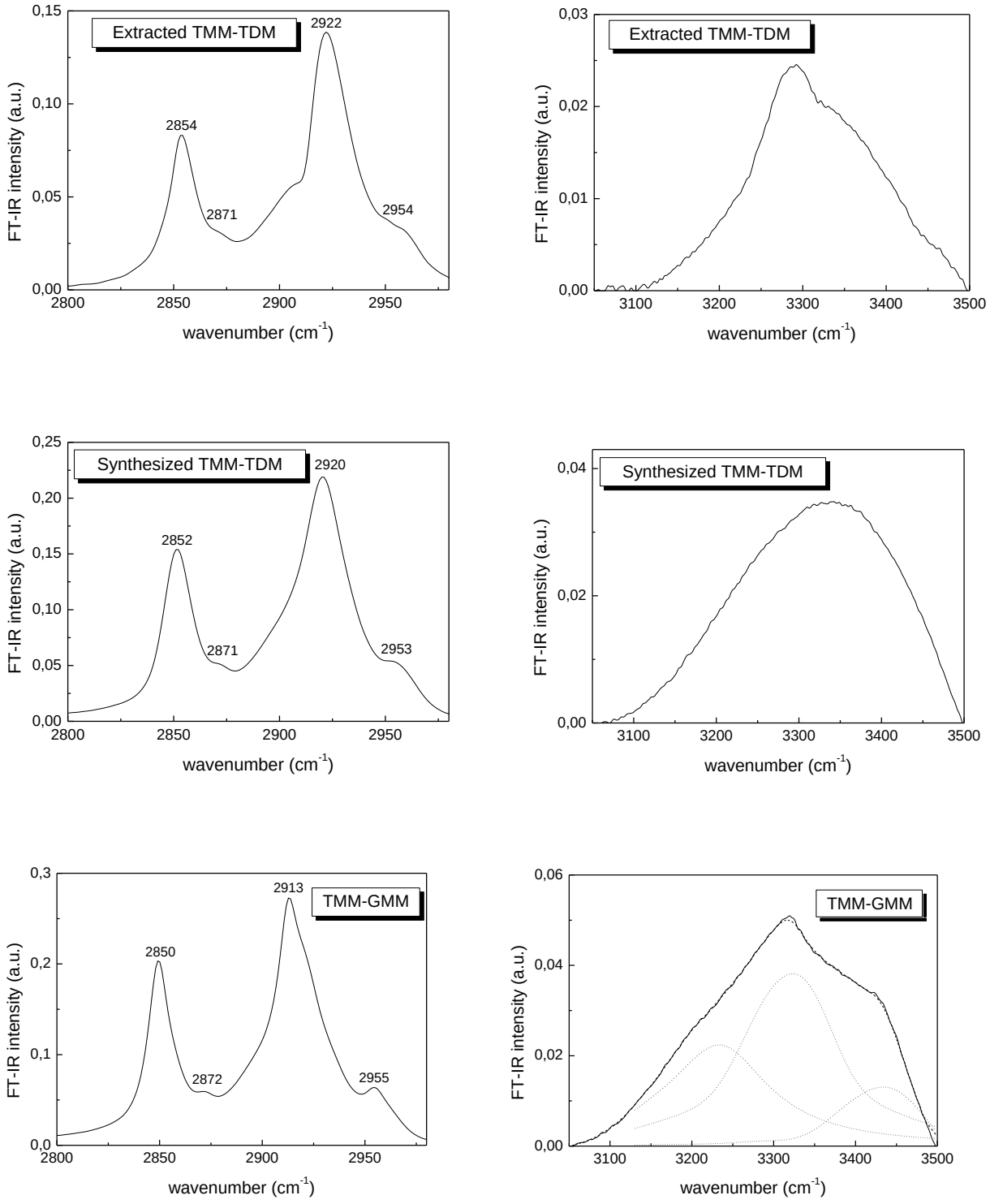

Figure 10. 2800-3500 cm^{-1} region of FT-IR spectra of synthesized and extracted TMM/TDM and TMM/GMM with the CH_2 asymmetric and symmetric stretching modes and the CH_3 asymmetric and symmetric stretching. In the TMM/GMM spectrum in b) the deconvolution result is shown.

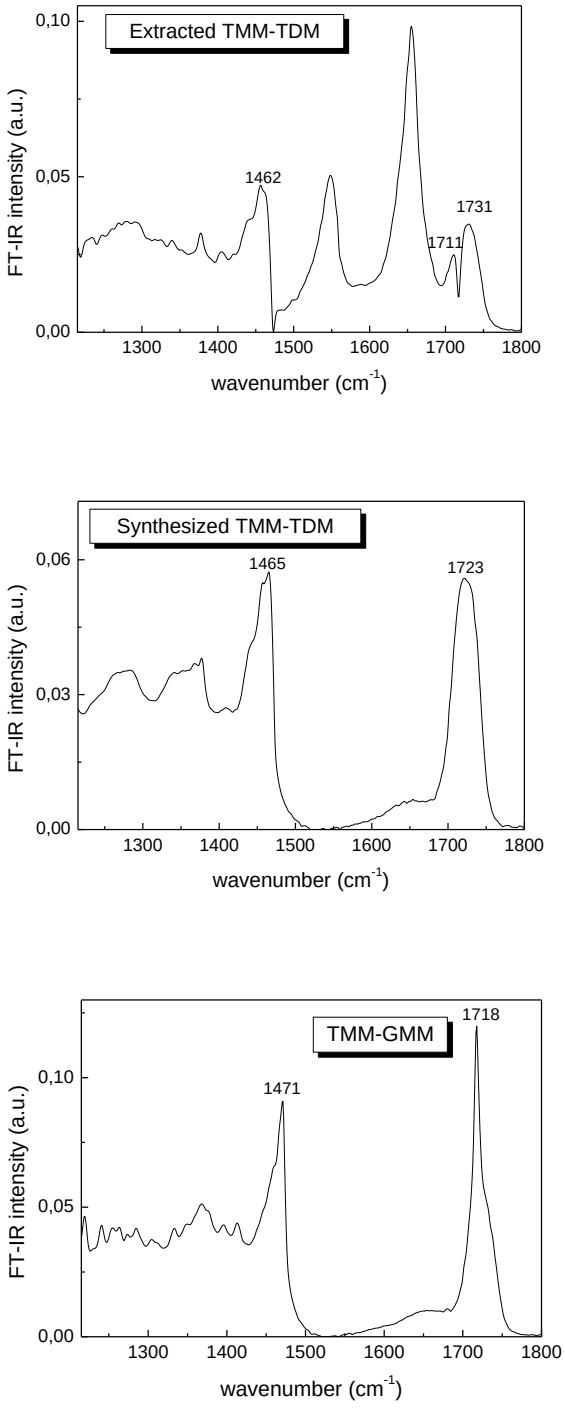

Figure 11. 1215-1800 cm^{-1} region of FT-IR spectra of FT-IR spectra of synthesized and extracted TMM/TDM and TMM/GMM with the C=O stretching modes and the CH_2 scissoring modes

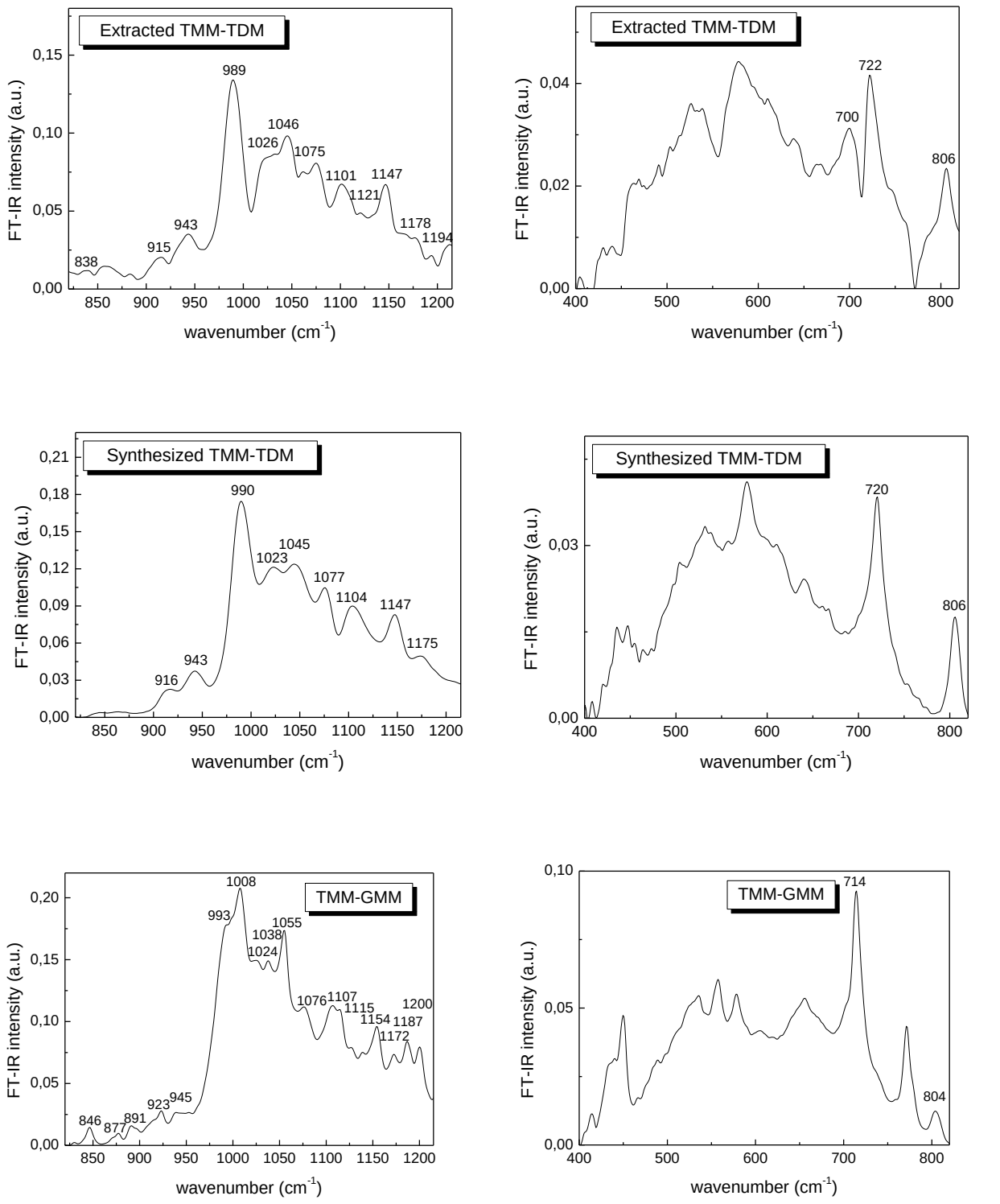

Figure 12. 400-1215 cm^{-1} region of FT-IR spectra of synthesized and extracted TMM/TDM and TMM/GMM with the C-O asymmetric and symmetric stretching modes, the C-C stretching modes and the C-H rocking modes

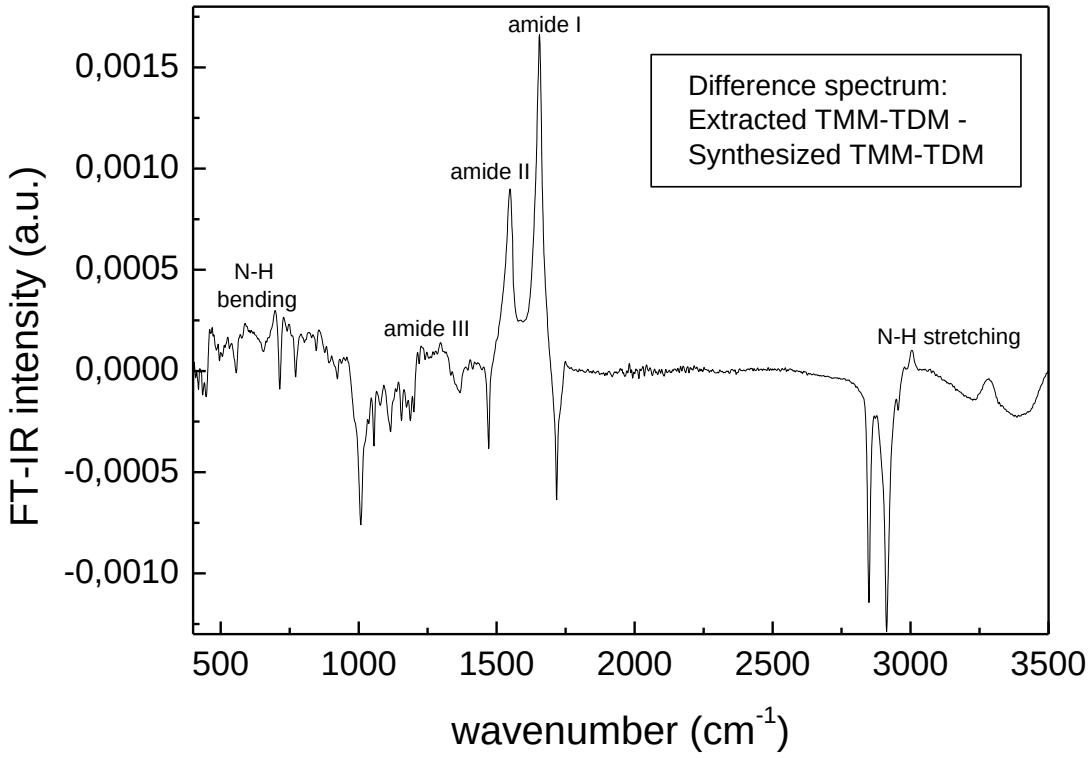

Figure 13. Difference spectrum obtained by subtracting the synthesized TMM/TDM spectrum from the extracted TMM/TDM spectrum with the protein spectral contributions

Table 1. Mode assignment for the FT-IR frequency values in TMM, TDM, GMM, extracted TMM-TDM, synthesized TMM-TDM and TMM-GMM

FT-IR modes	**TMM position (cm^{-1})**	**TDM position (cm^{-1})**	**GMM position (cm^{-1})**	**extracted TMM-TDM position (cm^{-1})**	**synthesized TMM-TDM position (cm^{-1})**	**TMM-GMM position (cm^{-1})**
OH stretching – CO-NH-peptide	3310	3333	3426 3316	3333 3290	3331	3395 3319
CH_3 asymmetric stretching	2955	2954	2955	2954	2953	2955
CH_2 asymmetric stretching	2920	2920	2912	2922	2920	2913
CH_3 symmetric stretching	2870	2871	2871	2871	2871	2872
CH_2 symmetric stretching	2851	2851	2849	2854	2852	2850
C=O stretching	1719	1724	1718	1731 1711	1723	1718
amide I				1658		
amide II				1548		
CH_2 scissoring	1462 1413	1466	1471 1413	1462	1465	1471
CH_3 symmetric bending		1377		1377	1376	
CH_2 wagging CH_3 asymmetric bending		1368 1355 1339	1367	 1340	 1340	1369 1334
CH_2 wagging – CH_2 twisting	1271	1278	1286	1279	1273	1285
amide III				1230-1300		
C-O asymmetric stretching - C-O-C bridging	 1146 1107	 1175 1147 1118 1104	1200 1187 1173 1156 1115 1109	1194 1178 1147 1121 1101	 1175 1147 1104	1200 1187 1172 1154 1115 1107
C-O symmetric stretching - C-O-C non-bridging	1076 1050 1032	1074 1050 1021	(1077) 1055 1039	1075 1046 1026	1077 1045 1023	1076 1055 1038 1024
C-C stretching	989	992	1007	989	990	1008 993
C-C stretching – C-H rocking	942 864	945 916 845		943 915 838	943 916	945 923 891 877 846
“fingerprint” region	805 722	806 721	713	806 722 700	806 720	804 714

Graphical abstract